IMPLEMENTATION OF SOLAR ENERGY IN URBAN PLANNING

Analysis of $SAFAR_n$ as a solar potential metric & improvement of simulation tools

Mihail Todorov

Master thesis in Energy-efficient and Environmental Buildings
Faculty of Engineering | Lund University

Lund University

Lund University, with eight faculties and a number of research centres and specialized institutes, is the largest establishment for research and higher education in Scandinavia. The main part of the University is situated in the small city of Lund which has about 112 000 inhabitants. A number of departments for research and education are, however, located in Malmö. Lund University was founded in 1666 and has today a total staff of 6 000 employees and 47 000 students attending 280 degree programmes and 2 300 subject courses offered by 63 departments.

Master Programme in Energy-efficient and Environmental Building Design

This international programme provides knowledge, skills and competencies within the area of energy-efficient and environmental building design in cold climates. The goal is to train highly skilled professionals, who will significantly contribute to and influence the design, building or renovation of energy-efficient buildings, taking into consideration the architecture and environment, the inhabitants' behaviour and needs, their health and comfort as well as the overall economy.

The degree project is the final part of the master programme leading to a Master of Science (120 credits) in Energy-efficient and Environmental Buildings.

Supervisor: Jouri Kanters
Examiner: Maria Wall

Keywords: solar potential, SAFAR, photovoltaics, assessment tool, NZEB, urban planning, solar energy

Thesis: EEBD - # / YY

Abstract

The increasing concern for buildings' energy use, emphasizes on the importance of implementation of renewable energy sources such as solar energy. However, currently there is not enough knowledge amongst the actors involved in urban planning of the cities regarding the effect of their decisions on the solar potential of buildings. Therefore, the development of methods and tools for assessing the solar potential of buildings and encouraging the implementation of solar energy are necessary.

Targeting this issue, the study looks into the further development of the solar potential metric $SAFAR_n$ by testing it on real case buildings in Hyllie, Malmö. The results revealed that buildings possess a great potential for solar energy harvesting and the most suitable area to that is the roof. Furthermore, the building density and compactness ratio proved to be a determining factor for the $SAFAR_n$.

The study also assessed the effect of the surroundings, represented by different street width, neighbouring building heights and their facade materials on a building's solar potential. The results showed that larger street widths are more beneficial for the solar access. Additionally, the facades are very susceptible to shading, as for the roof a large difference in the suitable area and load coverage between a higher or a lower solar irradiation threshold was observed. The reflectance of the materials also proved to have a certain contribution to the solar irradiation on the building envelope.

Moreover, a building assessment tool for solar energy design based on the program Grasshopper was developed in order to assist urban planners and architects to take more informed decisions during early design stage. The tool proved to be capable of providing predictions about the amount and the location of a building's suitable area, placement and size of the solar energy system, as well as the amount of electricity that the system can produce and subsequently how much of the building's electricity need can be covered. The tool was also able to provide adequate visual and numerical feedback on the results. Additionally, the tool was demonstrated and validated following a step-by-step workflow performed on theoretical building block.

Acknowledgements

Table of content

Nomenclature

PV - photovoltaics, i.e. electric power generation with solar cells.

EDP – early design phase

NZEB – nearly zero energy building

IEA – International Energy Agency

$SAFAR_n$ – suitable area to floor area ratio

FSI – floor space index

BBR – Swedish Building Regulations

FEBY 12 - Requirements for Zero energy buildings, Passive houses and Minienergy houses issued by FEBY

ST – solar thermal, i.e solar thermal energy system

Terms and definitions

Ambient bounces (-ab): describes the maximum number of diffuse bounces computed by the indirect calculation. A value of zero implies no indirect calculation.

Ambient divisions (-ad): determines the number of sample rays that are sent out from a surface point during an ambient calculation. The higher the number the more accurate the results will be.

Ambient resolution (-ar): determines the maximum density of ambient values used in interpolation. Error will start to increase on surfaces spaced closer than the scene size divided by the ambient resolution

Ambient super-samples (-as): determines the number of extra rays that are sent in sample areas with a high brightness gradient. They are applied only to the ambient divisions that show a significant change.

Ambient accuracy (-aa): equals the error from indirect illuminance interpolation. A value of zero implies no interpolation

Monte Carlo method: statistical evaluation of mathematical functions using random samples in order to estimate parameters of an unknown distribution by statistical simulation.

Perez Sky model: a mathematical model used to describe the relative luminance distribution of the sky dome by using real data gathered from weather stations all over the world.

Ray-Tracing: a technique for rendering three-dimensional graphics with very complex light interactions. Ray tracing operates pixel-by-pixel following the path that light takes as it bounces through an environment.

1 Introduction

1.1 Background

Currently, over a half of the world's population resides in urban areas and this ratio is expected to increase to 66% by 2050 (UN, 2014). This trend of urban population growth has consequences on increased energy consumption, carbon dioxide emissions and increase of the effect of urban heat island in cities (UN, 2014). Buildings represent the largest energy-consuming sector, accounting for over one-third of the final energy and half of the electricity consumption on a global scale, which also results in approximately one-third of the global greenhouse gas emissions (IEA, 2013). For this reason, improving old and new buildings' energy efficiency by reducing their energy demand (for example the passive house concept), effectively utilizing the passive solar gains and daylighting, as well as using a larger fraction of renewable energy sources integrated in the urban context is necessary in order to create more sustainable urban environment (IEA, 2015).

According to the European Performance of Building Directives (EPBD), adopted by the European Parliament and the Council of the European Union, by the end of 2020 all new buildings in the European Union will have to consume nearly zero-energy, as well as existing buildings to undergo cost-effective refurbishment into nearly zero-energy buildings (European Parliament, 2010). In order to achieve this goal a significant part of the used energy should be provided by local renewable sources if possible (European Parliament, 2010).

One of the solutions for providing renewable energy locally is to integrate solar energy systems in buildings. Looking into this issue, for a number of years now international initiatives such as the IEA Solar Heating and Cooling Programme (IEA-SHC) are dealing with the development of research projects examining various aspects of solar energy use for heating, cooling or electricity, mainly regarding buildings (IEA-SHC, 2015). POLIS is a European project and a cooperation between several cities in Europe with a focus on implementing strategic town planning and local policy measures for solar energy utilization in European cities (Intelligent Energy Europe, 2012).

However, there are some of the constraints for implementing solar energy systems in urban contexts such as the reduction of direct solar energy (surrounding buildings or other objects casting a shadow, unsuitable surface orientation) and the limited surface area (roof and facade) per floor area. According to Kanters (2015), proper solar radiation utilization could be ensured with preliminary analyses during the early design phase (EDP) on building size, form, orientation, overshadowing, as the solar potential for harvesting solar energy on building surfaces would be improved. Decisions taken during the EDP evidently have a great impact on the following phases and the performance of the building (Biesbroek et al., 2010; Kanters & Horvat, 2012). This means that important players from the building sector, such as urban planners, architects and engineers, should be able to make well-informed decisions in

the very beginning, in order not to put constraints on the solar potential of the buildings' further in the design phase.

Early design decisions are normally taken when preparations of a zoning plan are made. The zoning plan is a legal instrument for urban planners to set up certain boundaries of the use of land, street dimensions, open spaces, density of the buildings, the buildings' function, orientation, height and roof type (Kanters & Wall, 2014). Therefore, these decisions set up early in the process of development of an area, directly affect the potential for solar energy of the buildings (Kanters et al., 2012a). As indicated by Kanters & Wall (2014), currently there is limited knowledge of the amount of energy that on-site renewable energy sources can cover in relation to the annual energy demand in buildings, as well as the effect of urban planners' decisions on the solar potential of buildings. For this reason a new solar potential metric $SAFAR_n$ was introduced, which expresses the ratio between the suitable area on the building envelope and the total floor area of the building (Kanters & Wall, 2014). The base concept of the metric is to assess how much suitable area (roof and facade) a building has and to locate where this area is, in order to place a solar energy system, which would afterwards lead to an estimation of a possible production and energy coverage (Kanters & Wall, 2014). $SAFAR_n$ is intended to assist urban planners with taking well-informed decisions for solar energy when preparing the zoning plan, as well as to provoke real estate developers to consider solar energy for their buildings (Kanters & Wall, 2014).

In order to take the right decisions for solar energy, methods of quantifying the solar potential and tools for performing these calculations that would present necessary information for each involved actor are needed. As a part of IEA-SHC Task 41: Solar Energy and Architecture, an international survey targeted towards practicing architects was conducted, with intentions to address issues related to passive and active solar design, as well as the adequacy of the existing digital tools for architectural integration of solar energy (Kanters et al., 2012b). Amongst other issues the outcome of this study indicated that the methods architects use did not support their decision-making process and their knowledge about solar energy technologies is not high (see Figure 1.1). The study also indicated that there are many advanced tools suitable for detailed design phase that are too complex, too expensive, not well incorporated into the workflow of the architects and lack interoperability with other commonly used software such as CAD (Kanters et al., 2012b). A lack of well-developed conceptual design tools for solar design at EDP that would provide key data for preliminary sizing of the solar energy system by means of numerical and visual output was also indicated (Kanters et al., 2012b).
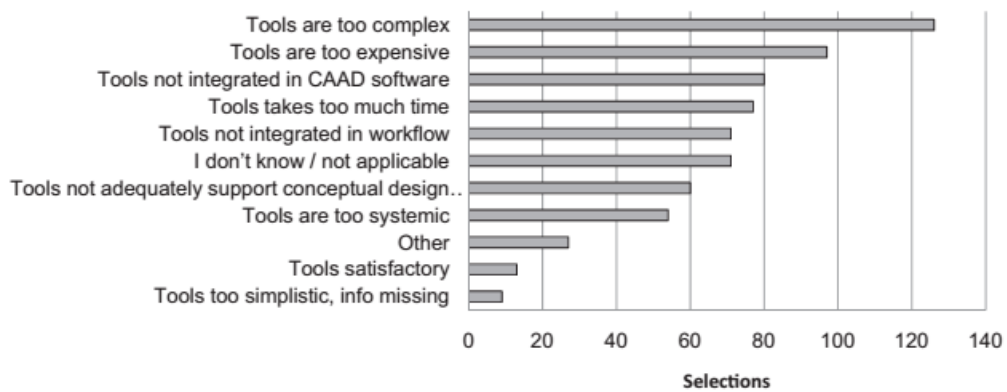
Figure 1.1 Barrier of available tools for architectural integration of solar design (Kanters et al., 2012b)

Architects, urban planners and real estate developers are important actors in cities development process, therefore, it is of high importance that they understand their impact on the solar energy potential of the buildings (Kanters & Wall, 2014). The development of better tools and methods is necessary for improving the quality of the decisions taken during the design process. Therefore, this research targets this issue and aims to bring further knowledge of the solar potential metric $SAFAR_n$ and introduces a new solar assessment tool.

1.2 Research aims

This research is related to IEA SHC Task 51: Solar Energy in Urban Planning, which is a part of The Solar Heating and Cooling Programme (SHC), established by the International Energy Agency in order to enhance and promote the use of solar energy (IEA, 2015). The core of Task 51 is to provide ways to support the urban planners, architects, real estate developers and authorities to successfully implement solar energy in urban planning for achieving urban areas and whole cities with a large fraction of renewable energy sources (IEA, 2015). The overall aim of this research is to provide more support for the key actors of urban planning regarding solar energy implementation. This study is divided into two parts focusing on $SAFAR_n$ metric and solar energy building assessment tool.

1.2.1 Suitable Area to Floor Area Ratio ($SAFAR_n$)

The aim of this first part of the study is to bring further knowledge to the solar potential metric $SAFAR_n$, which was introduced by Kanters & Wall (2014). In their study, Kanters & Wall (2014) partly looked into the effect of an early urban planning design decisions, where form (based on a southern Sweden building typology), density, orientation and roof type were examined.

The first step of this part of the study looks into a case study in Hyllie, Malmö of an already planned urban district. The aim is to test the $SAFAR_n$-method on real case buildings, chosen according to their different surrounding context and to investigate the relationship

between solar potential, building form and density. Additionally, the potential for solar electricity production and the subsequent load coverage were investigated.

In the second step of this part, the research project aims to examine the effect of the surroundings on the solar potential ($SAFAR_n$) in a theoretical urban setup, typical for cities in southern Sweden (Skåne) and similar to the buildings selected in the Hyllie case study. Parameters such as street width, neighbouring building height and buildings' facade surface materials are examined. The results should enhance the knowledge of how surroundings affect buildings' suitable area for installing PV panels and provide helpful insights for taking solar energy into account during planning phase.

1.2.2   Solar energy building assessment tool

The primary aim of this second part of the study is to develop a Grasshopper-based building assessment tool for solar energy design during early design phase, which provides visual and numerical information about solar energy generation, load coverage, system size and placement, necessary for assessing the solar potential of a building. The second part of this study part aims to demonstrate the tool by the use of a step-by-step process, where an assessment of a theoretical building within an urban setup featuring a diverse surrounding context is performed.

1.3   Scope and limitations

This study focuses on investigating the solar potential metric SAFAR, which is primary dependent on predetermined solar irradiation thresholds. Even though the metric SAFAR is aimed to be adaptable for international purposes, the chosen thresholds were adapted to the context of Southern Sweden (Skåne region) where this study was focused on. The results of this study can be mainly applicable in regions with similar landscape and climate characteristics. However, the pre-determined solar irradiation can be adapted according to the location and all simulations can be executed as long as the correct weather data is applied. Therefore, the methodology of this solar potential study could be used all over the world.

The research limits its scope to investigating solar potential for solar photovoltaic (PV) systems and does not take into consideration other types of solar systems. Therefore, the research results regarding SAFAR can be applicable mainly in assessing solar potential for PV systems. However, with some modifications, the results regarding solar energy building assessment tool could also be applied in other than PV systems.

The Grasshopper-based solar design tool developed in this study is able to calculate the hourly production per panel for a pre-defined period of time. The hourly results are especially useful when calculating the financial benefit of a photovoltaic solar energy system. However, this study does not encompass financial aspects of the solar energy systems and does not implement any calculations regarding the feasibility of the system, which creates a gap for future research in the study field.

Another limitation of the research is its focus on residential buildings, as an analysis of different purpose buildings might require some adjustments and deliver different results. Moreover, due to the time limitations of this project, the script could not be developed to its full potential in order to determine the best setup of the PV panels. Even though the purpose of the study was to demonstrate and test the tool, due to the time limit, no alterations or optimizations in the building design were made in order to provide more thorough overview of the tool.

2 Theoretical framework

The following chapter builds up the theoretical knowledge that is important for the development of the research. Therefore, the concepts of solar energy and urban morphology are introduced and discussed in detail. Furthermore, previous research of solar potential in an urban context, as well as electricity use and production in buildings is analysed and discussed.

2.1 Solar energy

The average solar radiation towards the earth on average is 1367 W/m^2 but due to absorption or scattering of molecules in the atmosphere, the maximum level that reaches the earth is 1000 W/m^2 (Beckman & Duffie, 1991). The solar radiation towards a horizontal plane is typically divided into direct, diffuse and ground reflected radiation, where direct radiation is the radiation that is not intercepted by any obstructions or clouds and diffuse radiation is blocked by clouds and objects and then reflected (Beckman & Duffie, 1991). Radiation that is reflected from the ground is called ground reflected radiation. The diffuse and ground reflected radiation vary depending on the reflectance properties of the surface. The fourth type of radiation is the circumsolar diffuse radiation (occurs when a surface is tilted) (see Figure 2.1), which comes from the same direction that the direct beam does (Beckman & Duffie, 1991), but it is scattered by water vapour and aerosols in the atmosphere.
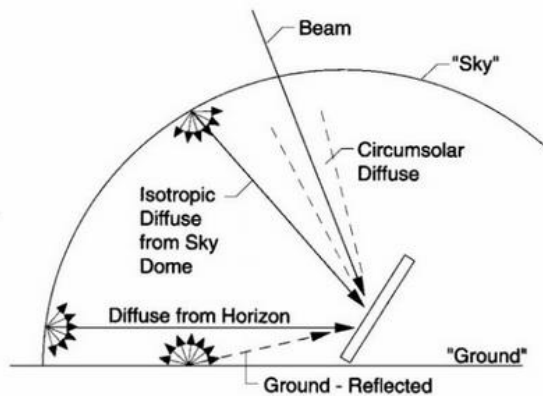

Figure 2.1 Solar radiation types towards a tilted surface (Beckman & Duffie, 1991)

2.1.1 Solar irradiation

The solar irradiation towards a horizontal or inclined surface differs depending on the latitude. Compared to countries located in southern Europe, Sweden has significantly lower potential for solar electricity, as it is shown in Figure 2.2. However, the amount of irradiation does not differ that much than countries located in central Europe, such as Germany, which are leading the market of PV capacity in the European Union, but the installed capacity is much less (IEA-PVPS, 2014). In southern Sweden (Skåne region), where this research is focused, the amount of global solar irradiation on average is 962 kWh/m^2 and the solar

irradiation on an optimally inclined surface is approximately 1150 kWh/m^2 and an optimum inclination angle is 41° (PVGIS, 2015). This amount of solar energy can be utilized in the buildings in a passive way as daylight and passive solar gains, and in an active way using PV panels and ST collectors.
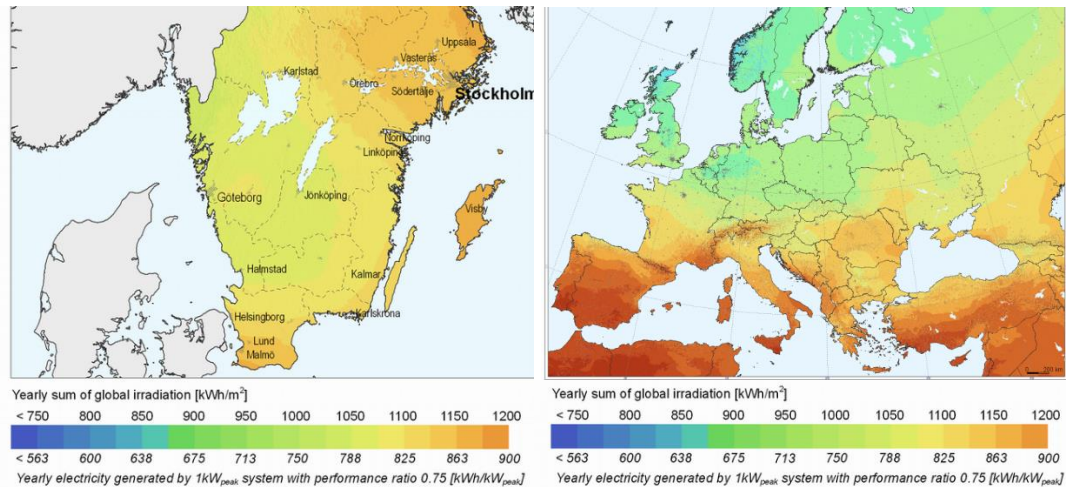

Figure 2.2 Solar irradiation on optimally inclined surface in Sweden and Europe (PVGIS, 2015)

2.1.2 The photovoltaic technology

The photovoltaic effect is a direct conversion of light into direct current electricity using a PV panel (IEA-PVPS, 2014). The PV system consists of one or more PV modules connected either directly to the electricity load (off-grid), either to the electricity network (grid-connected) (IEA-PVPS, 2014). Apart from the PV modules, in most cases the system consists of an inverter to convert the power from a direct current (DC) to an alternating current (AC) in order to be able to utilize the generated electricity. If the system is off-grid, then a storage battery is required in order to provide electricity during periods with low or no solar radiation (IEA-PVPS, 2014). If the system is grid-connected, then a storage battery is not required, as long as the unused electricity can be fed-in to the grid (IEA-PVPS, 2014).

In an urban environment, PV systems are normally connected to the electricity grid. Their application or integration in buildings is steadily growing, especially for building integrated PV systems (BIPV), placed on the facades, opaque or semi-transparent glass-glass, shading device integration, different types of roofs, PV roof tiles (IEA-PVPS, 2014). However, according to IEA-SHC Task 41 (2013), one of the main barriers for implementing PVs in buildings is the lack of architecturally attractive products, which implies for further developments to improve the flexibility in size, colour, and surface texture which would increase the attractiveness of the PV products.

There are several types of PV panels, with varying efficiency and cost, however the most commonly used, representing the largest fraction of the PV cells market are the

crystalline silicon cells with efficiency between 15-20% (IEA-PVPS, 2014). In an urban context the panels can be shaded by surrounding buildings, by protruding chimneys, vegetation or other objects, which could lead to significant loss in efficiency, which consequently would decrease the output. This due to the fact that the cells inside the module are connected in series, which means that if a cell is shaded this will lead to current failure in the whole string (Gomes et al., 2013). In order to reduce the effect of shading, bypass diodes can be used to redirect the current to flow in another path and thus allow for the other cells to operate (Gomes et al., 2013).

Another cause of shading that needs to be considered is the mutual shading of the panels when placed on a flat roof. Kanters & Davidsson (2014) performed a study on the total solar potential and economic consequences of mutual shading of PV systems, where they examined different tilts and row spaces of the panels in Lund, Sweden. The research revealed that the effect of mutual shading significantly reduces the output of a model when the row distance is smaller than 1m (Kanters & Davidsson, 2014). It was also concluded that the maximum annual energy output of a flat roof is reached when the system had an inclination of 0° and row distance of 0 m, due to the fact that there is no overshadowing, as well as due to lack of distance between the panels lead to a greater system size. However, such inclination is not practically possible because introduces problems of snow and rain runoff (Kanters & Davidsson, 2014). Additionally, inspection and maintenance is not possible, due to the lack of row spacing. Based on current electricity prices, the shortest payback time of a system was registered to be at an inclination of 30° for Lund, which resulted in a smaller system size and subsequently smaller electricity output (Kanters & Davidsson, 2014).

A high ambient temperature and solar radiation heating up the PV panel have a negative effects on its efficiency and its production (Gomes et al., 2013). With an increased panel temperature the band gap becomes smaller and the extraction of voltage is reduced, leading to a decrease in the cell efficiency (Gomes et al., 2013). Figure 2.3 shows how the IV-curve, which illustrates how a specific cell behaves under different resistance levels at a certain condition and when it is affected by the different irradiation and temperature (Bernardo, 2013). The whole system is also subjected to other losses such as inverter losses, DC and AC cable losses, soiling and others (NREL, 2015).
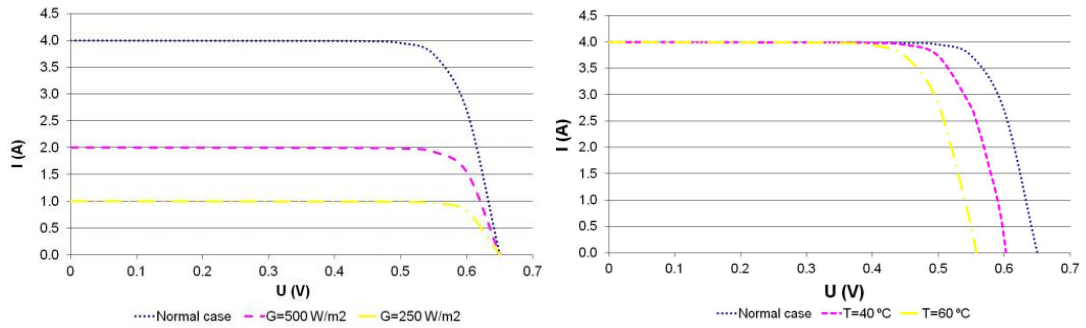
Figure 2.3 I-V curves and power outputs for different irradiation and temperatures (Bernardo, 2013)

2.2 Urban morphology

Urban morphological indicators are used to analyse physical structures at different scale such as building form, street pattern, plot pattern and other (Anderson et al., 1996). On a building level, these indicators can be used to compare different building typologies (Anderson et. al, 1996). In this research the following urban morphology metrics are implemented in order to describe and compare the solar potential of the examined cases.

2.2.1 Urban density

Urban density is an important parameter for urban planners regarding sustainability in cities. Increasing the density in cities reduces the energy for transportation, as well as optimizes the land use, however, building density also directly affects the solar access and daylight, what consequently leads to an increase in the heating demand and use of artificial lighting (O'Brien et. al, 2010) . Therefore, considering building density at the early design phase is important for creating a balance between solar access, daylight and energy use.

As it is represented in the Equation 1 , a common way to present the density is the Floor Space Index (FSI), or Exploateringstal kvarter in Swedish, which is the total gross floor area (TFA; m^2) divided by the plot area (A$_{plot}$; m^2) (Larsvall et al., 2010).

$$FSI = TFA/A_{plot}$$

Equation 1

Based on a study of an urban planning in Malmö (Larsvall et al., 2010), the area of the plot (Swedish: Exploateringsyta, Ey) is calculated by adding together the land area (Tomtyta, Ty) and the area that represents half of surrounding streets or a park (Omgivande gata, park och kaj, Gy) (see Figure 2.4). Additionally, if the adjacent street or park is larger than 30m, then a fixed distance of 15m is taken (Larsvall et al., 2010). This way the density of a building represents the area that is exploited by the building owner.
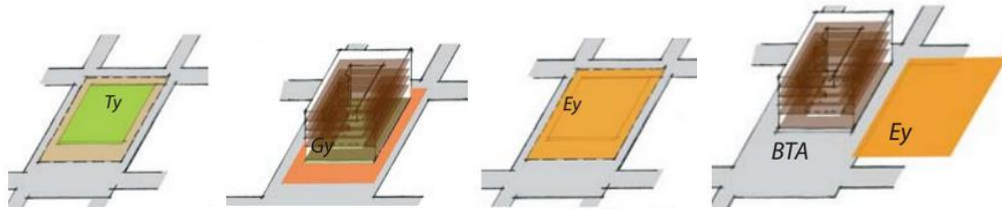
Figure 2.4 Density and plot ratio expression

Figure 2.5 shows that the FSI can be expressed in a different way depending on the geometry of the building. For example, when FSI=0 the plot is empty. When the FSI=1, this means that the whole plot is built with a one-storey building. If the FSI=2, this means that the whole plot is occupied by a two-storey building or half of the plot by a four-storey building and etc.
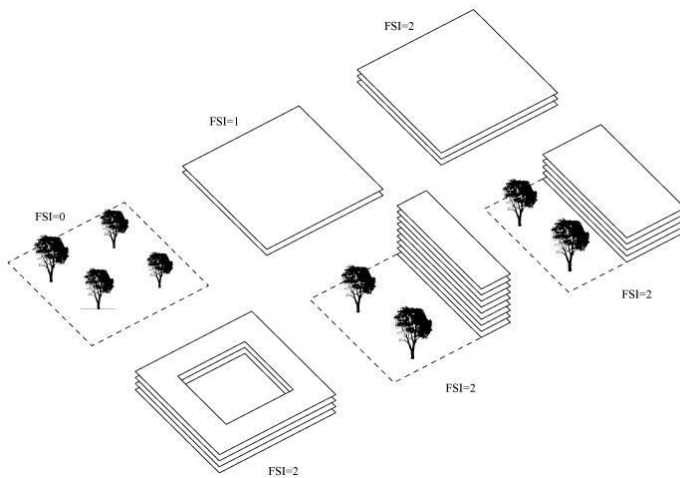

Figure 2.5 FSI (Solar planning, 2015)

2.2.2 Compactness ratio

Compactness ratio (Comp) of a building is a metric counted as the ratio between the total external envelope area (Env; m^2) in proportion to the total floor area (TFA; m^2) of the building (see Equation 2) (Álvarez, 2013).

$$Comp = Env/TFA$$

Equation 2

Compactness ratio can be used to get more understanding of the energy performance and it expresses the total external envelope area in proportion to the total floor area of the building (Álvarez, 2013). Lower values correspond to a more compact building, which leads to lower heat flow through the envelope. In terms of solar potential, this metric has a reversed effect compared to energy performance, as the more compact a building is, the less envelope

17

area is available, thus the solar potential of the building is decreased (Sattrup & Strømann-Andersen, 2013).

2.2.3 Street width

In an urban context buildings overshadow and limit one another's daylight and solar access, due to the restricted space between them. Since streets most often represent this space, their width is an important parameter for urban planners to consider. According to a study carried by Larsvall et al. (2010) that examines Malmö's urban planning, several types of street widths are identified, depending on the function, traffic load and vegetation (see Table 2.1). A main street is classified as a road to a neighbourhood that would provide good accessibility for cars, public transport, emergency vehicles, etc., as well as separate paths for pedestrians and cyclists (Larsvall et al., 2010). "Uppsamlingsgata" (see Figure 2.6) stands for a road that has a two-way road with one lane for each direction, separate paths for cyclists and pedestrians and planting (Larsvall et al., 2010). A local street is a street in-between the building blocks and the smallest type of road is classified as an alley, where pedestrians and cars share (Larsvall et al., 2010).

Table 2.1 Example of street types in Västra Hamnen, Malmö

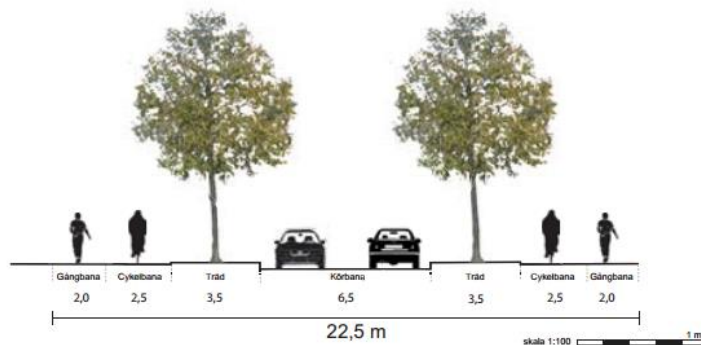|	Main street	"Uppsaml ingsgata" + trees	"Uppsaml ingsgata"	Local street + trees	Local street	Alley
Width / (m)	33	26	22.5	14	11	8-9

Figure 2.6 Example of "Uppsamlingsgata"

2.3 Solar potential in an urban context

Urban context provides a complex environment, which presents many obstacles and opportunities for utilization of solar energy. In order to evaluate the potential for solar energy of a city, a district or a building block, certain methods and tools are necessary to be able to give numerical and visual output, which would be determining for decisions taken by authorities, urban planners and other involved actors (Kanters, 2015).

18

Compagnon (2004) presented a method for quantifying the solar potential of the external envelope of buildings located in urban areas for active and passive heating, photovoltaic electricity production and daylighting. The study also presented the setup of threshold values for the above mentioned techniques (see Table 2.2). These thresholds were determined on a basis of current technology limitations and economic considerations (Compagnon, 2004). In terms of potential for Solar Thermal (ST) and PV systems, the thresholds indicate the minimum amount of solar radiation on a surface that would be suitable for installing a solar energy system (Compagnon, 2004). This method enables an early design phase analysis that can determine a building's solar potential for installing a solar energy system (Compagnon, 2004). However, as indicated by Kanters & Wall (2014), Compagnon's thresholds are based on a specific location and in other regions of Europe they would probably differ.

Table 2.2 Threshold values for the corresponding solar techniques (Compagnon, 2004)

Solar technique	Threshold for facade systems	Threshold for roof systems
Passive thermal heating	216 kWh/m^2 (heating season)	Same as for facades
Photovoltaic systems	800 kWh/m^2 (annual)	1000 kWh/m^2 (annual)
Solar thermal collectors	400 kWh/m^2 (annnual)	600 kWh/m^2 (annnual)
Daylighting systems	10 klx mean illuminance (8h-18h)	Same as for facades

Kanters & Wall (2014) introduced thresholds applicable in a Swedish context, based on categories used in Lund's solar map (see Table 2.3). $SAFAR_n$ could be measured for any of the thresholds described above ("n" represents the solar radiation threshold value in kWh/m^2a), but it will be more logical to exlcude the "unsuitable" category (Kanters & Wall, 2014).

Table 2.3 Threshold values for different categories / (kWh/m^2a) (Kanters & Wall, 2014)

	Unsuitable	Suitable		
		Reasonbale	Good	Very Good
Facades	0-650	651-899	900-1020	> 1020
Roof	< 800	800-899	900-1020	> 1020

By using Radiance through DIVA-for-Grasshopper, Kanters & Wall (2014) tested the solar potential metric for four building blocks typical for southern Sweden, where they partly examined the effect of design decisions regarding building density, orientation and roof type. The results showed that building density was the most influential parameter on the solar potential, and for the highest solar energy production potential flat roofs and orientation between 15° and 60° showed to be the best (Kanters & Wall, 2014).

Cheng et al. (2006) examined the relationship between built form, density and solar potential, where generic models representing a combination of the two parametes were simulated. The assessment criteria were be the openness at ground level, daylight factor and

the PV potential on building facades (Cheng et al., 2006). The assessment was performed in PPF, a Radiance-based tool, digital elevation model (DEM), image processing of 3-D urban texture used to determine the sky view factor (SVF) at ground level (Cheng et al., 2006). In terms of PV potential, the evaluation was based on Compagnon's radiation thresholds (Cheng et al., 2006). For implication in high density cities the results indicated that horizontally scattered building blocks are more favourable than uniform arrays and as for higher buildings arrangement, less site coverage and more open spaces is preferable than lower buildings with high site coverage and respectively less open spaces (Cheng et al., 2006). As for the vertical layout, varying or even random building height have been found to be more favourable that, as the researchers indicated, could vary significantly with other random configuration of the layout (Cheng et al., 2006).

Van Esch et al. (2012) made a study on the effects of urban and building design parameters on the solar access and passive solar heat gains on the urban canopy. The investigated urban parameters included four street widths and two street and building orientations (Van Esch et al., 2012). As for the building design parameters, three roof types and two types of facade design were chosen (Van Esch et al., 2012). The study results showed that street width had a significant influence on the total global solar radiation yield of the urban canyon, however, the orientation of the streets did not influence the radiation yield but it made a difference in the distribution of radiation over the separate canyon surfaces (Van Esch et al., 2012). The roof shape proved to have a significant influence on the direct irradiation on the street surface and as for the façade, increasing the amount of windows will often lead to overheating in the summer (Van Esch et al., 2012).

One way of assessing the solar potential in existing urban context is the solar map that is based on a Geographic Information System (GIS) tool providing information on annual solar irradiation on building surfaces and possibly the output of a solar energy system (ST/PV) and Light Detection and Ranging data (LiDAR) (Nguyen, Ha T. et al, 2012). A study on solar maps was carried by Kanters et al., (2014), where the maps were classified into three categories of basic, medium and advanced, depending on the information that they provided as output. Jakubiec & Reinhart (2013) created an advanced photovoltaic potential map for the city of Cambridge, MA, USA, based on a new method they developed for predicting the electricity output from PV panels based on LiDAR and GIS data combined with hourly simulations in the building simulation program Daysim. Additionally, they also incorporated the effect of hourly roof temperatures in order to calculate the efficiency of the PV panels and their method was compared to real measured production and the results showed an error range of 3,6-5,3% (Jakubiec & Reinhart, 2013).

Kanters, Wall & Dubois (2012) introduced a facade assessment tool (FASSADE) for solar energy, based on the DIVA4Rhino plug-in. The tool combines simulation engines such as Radiance/Daysim and EnergyPlus for performing hourly solar irradiation calculations, used for the possible ST and PV production (Kanters, Wall & Dubois, 2012). The tool also

assesses the feasibility of the solar energy system by accounting for the local electricity and heat prices, as well as the investment costs and annual revenue for a payback time calculation (Kanters, Wall & Dubois, 2012). In order to demonstrate the tool, an analysis of a typical Swedish building block was carried out and the results indicated that shadowing of the facade surfaces caused by surrounding buildings affects the output of the solar energy system, which also results in longer payback time of the investment (Kanters, Wall & Dubois, 2012).

2.4 Electricity use and production in buildings

According to the Swedish Energy Agency (2013), electricity is the dominant energy used in Sweden with a total final electricity of 126 TWh in 2011, where the residential and service sectors were the largest consumers of electricity. Electricity is distributed by domestic electricity (household appliances, also known as plug loads), common electricity (elevators, general lighting, ventilation and pumps) and electrical heating (Swedish Energy Agency, 2013).

In the recent years buildings have been a major target for energy optimization that could be achieved by reducing the energy need of a building, as well as by providing energy through use of on-site renewable energy sources (Pless & Torcellini, 2010). When it comes to using solar energy as a renewable energy source, energy-policy makers and real estate developers are interested in the ratio of how much can the solar energy system contribute, on an annual basis, in relation to the consumed energy (electricity and heating) on an annual basis, represented by the solar fraction (Kanters & Wall, 2014). However, the annual solar fraction between produced and consumed energy does not show how much energy is consumed in reality. If the solar energy production is observed on an hourly basis for example, the difference between the need and the production would be very different during the night, when no solar production occurs.

In Sweden, the mandatory requirement for energy use in building is the Swedish building regulations, BBR 20 (Boverket, 2015). Another existing concept is the Passive House, which is a low energy concept that significantly reduces the need for energy in the building. In order to achieve the requirements a set of recommended strategies for design and construction are provided (SCN, 2012). Additionally, the Passive House in Sweden concept only focuses on reducing the energy and not on usage of renewable energy sources (SCN, 2012). The concept of NZEB (see Figure 2.7) defines that a building should use very low or nearly zero amount of energy annually that will be covered by a high fraction of locally installed renewable energy systems (European Parliament, 2010). According to the EPBD Directive, each member state has the freedom of quantifying the amount of energy need that would mean that there might be a big difference in the quantities between member states (European Parliament, 2010). The Swedish definition of NZEB will be implemented within the current building regulations, having only the consumption side legally binding, which creates a loophole in legal regulation (Kanters, 2015).
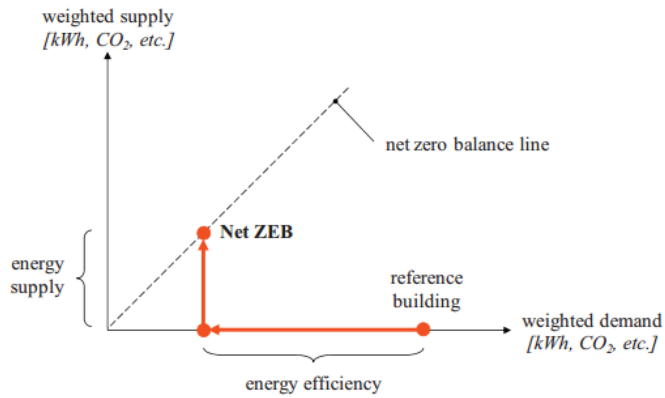
Figure 2.7 Net zero energy building principle (Sartori et al., 2012)

The current Swedish Building Regulations BBR give a total energy use demand of 90 kWh/m²a for the sum of space heating, domestic hot water and common electricity demand, for multi-storey residential buildings in climate zone III for Sweden (Boverket, 2015).

According to the voluntary criteria SVEBY (2012), if new residential buildings are planned, then 30 kWh/m²a should considered as a guideline value for the household electricity. In this research the examined buildings were assigned common electricity of 10 kWh/m²a (Kanters & Wall, 2014) and 30 kWh/m²a for domestic electricity, in order to assess their potential for covering the annual and hourly electricity load using solar energy.

3   Method

In order to fulfil the aims of this study, it was important to choose appropriate software as well as to make a pre-study on the Radiance parameters to determine their optimal proportion between accuracy and simulation time. Furthermore, necessary parameters and settings were needed to prepare for the following simulations and calculations. Further on the research method process was divided into two parts. The first part concentrates on the $SAFAR_n$ solar potential metric. The part consists of Grasshopper-based script development, $SAFAR_n$ real case study of Hyllie as well as analysis of how the solar potential of a theoretical building block is affected by different surrounding scenarios. The second part is focused on the solar energy building assessment tool. In this part of the study, a Grasshopper-based tool for solar energy design was developed and the tool's demonstration on a theoretical building was performed.

3.1   Software

Calculating $SAFAR_n$ and creating the Grasshopper-based tool for solar energy building assessment tool required the use of Rhinoceros software and its plug-ins such as Grasshopper, DIVA, Honeybee, TT-toolbox, Panelling tools and Horster.

Rhinoceros is a commercial 3-D computer graphics and computer-aided design software, based on NURBS mathematical model, which is used for modelling a wide variety of products, including architecture modelling (McNeel, 2015). It is a CAD software which uses Boundary Representation (Brep) to compose 3-D objects and be able to perform geometry manipulations (McNeel, 2015). Moreover, Breps allow solar irradiation and illuminance analysis through backward ray-tracing and radiosity techniques (McNeel, 2015). These capabilities and the widely-used CAD environment of the program would allow for a reliable import of 3-D geometry and interoperability between the main CAD tool and the building assessment tool described in this study. The tool's interoperability with CAD is a significant factor for its application in practise by architects, therefore, the research results could be easier implemented and used by them.

The Grasshopper plug-in is a graphical algorithm editor integrated within Rhinoceros 3-D CAD environment, which allows designers and architects to create complex forms without having knowledge of how to script (Grasshopper3d, 2015). The program allows a dynamic interaction with the 3-D geometry within Rhinoceros, where all manipulations made on the geometry are virtual and do not affect the actual imported model. Additionally, through the integration of free plug-ins in the program, such as DIVA and Honeybee, different environmental analyses on individual buildings or urban scale could be performed.

DIVA is an analysis tool integrated within both Rhinoceros and Grasshopper environments (DIVA-for-Rhino and DIVA-for-Grasshopper) (Jakubiec & Reinhart, 2011). Within DIVA, validated simulation engines such as Radiance, DAYSIM and EnergyPlus are

23

integrated that allow environmental evaluations such as climate-based solar irradiation, daylighting on a building or urban scale and energy use for single thermal zone (Jakubiec & Reinhart, 2011). To perform solar irradiation calculations DIVA combines Radiance and DAYSIM (Jakubiec & Reinhart, 2011). It first uses EPW annual climate data to subdivide the sky vault into 145 patches (Tregenza sky patches) and afterwards it generates the sky luminance/radiance from the centre point of each patch, with the use of the Perez sky model for each hour of the year (Robinson & Stone, 2004). Afterwards, using the GenCumulative Sky method it adds up all sky conditions for each hour of the year and stores the values in the 145 bins and in the end this cumulative sky is used in a Radiance (backward ray-tracing) calculation (Robinson & Stone, 2004).

In order to successfully run a simulation, the tool requires as input: geometry, an analysis grid (which subdivides the geometry into nodes (act as sensors on a surface), vectors (indicating the direction of the surface) and mesh faces (for visualization)), surface materials, a weather file and a time period for the analysis. Additionally, an important input for running the simulation is the Radiance settings that describe the calculation of inter reflected light and are crucial for the accuracy and duration of a simulation (Antonutto & McNeil, 2013).

Honeybee is an open-source Grasshopper plug-in for a full range of environmental analyses, integrating validated simulation engines such as Radiance, DAYSIM and EnergyPlus (Roudsari et al., 2013). The plug-in applies the same principle for the solar irradiation calculations as DIVA does (combines Radiance and DAYSIM to get the annual hourly irradiation), but through a Honeybee component the results for each hour of the year can be read in a more straightforward manner.

Additionally, free Grasshopper-based plug-ins of TT-toolbox, Paneling tools and Horster were used to create some of the features in the script that were not possible or needed more effort to achieve in the base environment of Grasshopper. TT toolbox created a link between Grasshopper and Microsoft Excel, in order to enable the export of data, generated as results of the simulations. Panelling tools was used to divide the building surface into a grid of sub-surfaces on which the solar radiation was calculated. The tool enabled for the formation of better division of these sub-surfaces at corners or irregular geometry. Horster was used to set up a camera view for visual presentation of the simulation results.

3.2 Radiance parameters

Radiance is the main program used to calculate the solar irradiation in this research. Setting of the Radiance parameters is crucial for the accuracy and simulation time of a calculation, therefore, a parametric study on Radiance parameters based on optimum accuracy and simulation time was performed. The study was carried out on a theoretical building surrounded by other identical buildings, where the solar irradiation on the roof and facade surfaces was calculated. As a first step a simulation based on a reference case settings, indicated as providing maximum accuracy (University of California, 1998) was carried out

(see Table 3.1). This was done in order to represent the building's solar irradiation in conditions closer to reality and to serve as a base for the following parametric study. The study was carried out in an iterative way, where one Radiance parameter at a time was changed (see Table 3.2). Each parameter was simulated five times, due to the Monte Carlo mathematical method used by Radiance, and then averaged in order to get the final value.

Table 3.1 Reference case settings and time of the simulations

	Radiance parameters				
	Ambient bounces (-ab) 8	Ambient divisions (-ad) 4096	Ambient super-sampling (-as) 2048	Ambient resolution (-ar) 1024	Ambient accuracy (-aa) 0.05
Time (min)	43				
Error (%)	-				

Table 3.2 A list of the evaluated Radiance parameters

-ab:	-ad:	-as:	-ar:	-aa:
2,3,4,5	512,1024,2048	128,256,512,1024	128,256,512,1024	0.1

The outcome of the study demonstrated that with higher values more accuracy was achieved, but also more time was needed in order to simulate. The results were obtained by calculating the relative error (%) between the results obtained from reference case settings (see Table 3.1) and the results from each parameter simulation (absolute error divided by known value). Figure 3.1 shows the outcome of the study, where the simulations for ambient bounces parameters showed that accuracy costs a lot of simulation time. However, the difference between 3 and 5 ambient bounces was around 1%, but the time needed was nearly double. The value of 2048 ambient divisions was chosen due to the best accuracy and an acceptable time lapse among the rest of the values. According to Ward & Shakespear (1998), ambient supersampling should be set to a half or one quarter of the ambient divisions value, therefore, 512 was selected as it demonstated an acceptaceble simulation time, compared to 1024 –as. As for ambient resulutions and ambient accuracy parameters 256 –ar and 0.1 –aa were selected, again due to acceptable time and error results.
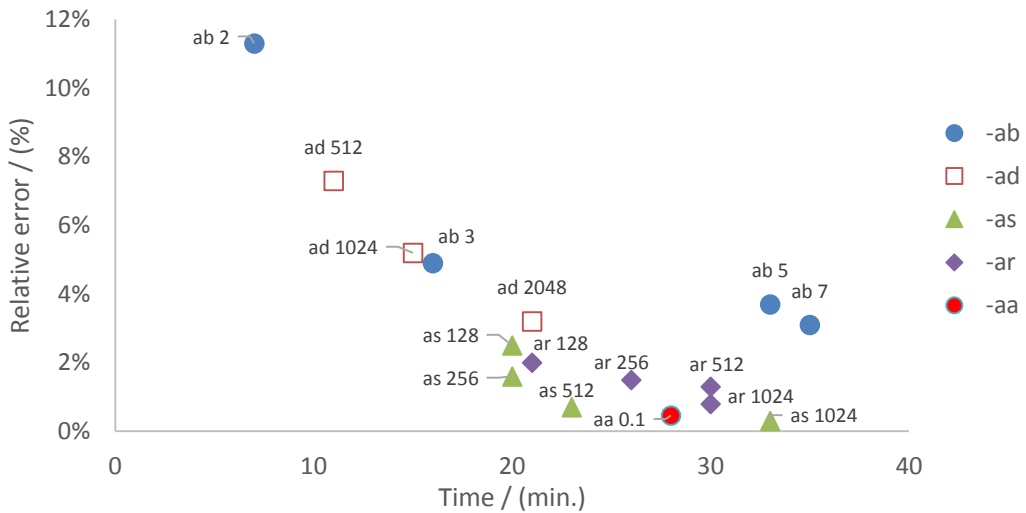
Figure 3.1 Parametric study on Radiance settings

The best case settings (-ab 3, -ad 2048, -as 512, -ar 256 and –aa 0.1) were then compared to the reference case and the results showed an acceptable error of 4% and greatly reduced time of 7 minutes for a simulation. It must be noted that the results for time in these simulations are also dependent on the computer characteristics.

3.3 Parameters and settings

In order to prepare the scripts for the solar analyses, a number of preconditions and parameters were considered. In the calculation for a building's floor area, every floor of the building was considered to have a fixed ceiling height of 3m for one storey, which also means that buildings with a ceiling height between 3 and 5m were still considered as one storey. Furthermore, parameters such as FSI and compactness were also calculated. The plot FSI was calculated by the ratio of the total floor area of the building to the area of the plot, which takes into account half of the adjacent streets, as well as up to 15m of distance if there is an open space adjacent to the building. In order to account for the openness around the examined building, the FSI of the surroundings was calculated by the sum of all surrounding building's floor area divided by the area of the examined land, which does not include the area of the plot. The compactness was calculated as the ratio between the total building envelope area to the total floor area.

All investigated buildings were located in Malmö, southern Sweden (Skåne region). However, Malmö city does not have a validated EPW weather file, therefore, the weather data for Copenhagen, Denmark, which is located at the same latitude and has a rather similar climate, was used instead. Furthermore, the buildings were modelled as simple volumes that exclude any balconies, chimneys or other protruding objects, since all models are at a planning stage where these kind of details are still unknown. However, in order to account for windows,

ventilation rooms, elevator shafts or other installations located on the roof, 25% of the available suitable area were excluded. It must be noted that the actual position of the windows and other installations was not specified. In the model all building surfaces (examined buildings and surrounding buildings) were designed with a reflectance of 35% and the ground surface with a reflectance of 20%, which are commonly used values solar radiation studies (Jakubiec & Reinhart, 2013). In order to account for the absorptive properties of the PV panel, a reflectance value of 10% was assumed for the solar energy assessment tool.

In order to quantify the solar potential of a buildings' surface, annual irradiation thresholds defining the suitable and unsuitable areas for installing a PV system were determined. The thresholds for roof and facades introduced by Compagnon (2004) and Kanters & Wall (2014) have been determined on the basis of economy and technology factors, where roofs are suggested with a higher threshold (800 kWh/m^{2}a) for suitable area than facades are. However, in this study a separation between roof and facade was not made, so as to investigate the full potential for load coverage and still be within the boundary of the suggested thresholds (considering 800 kWh/m^{2}a as a threshold for the roof will result in smaller suitable area). Therefore, all surfaces receiving irradiation equal or greater than 650 kWh/m^{2}a were considered suitable and any surface with irradiation below 650 kWh/m^{2}a was classified as unsuitable area (see Table 3.3). Based on these thresholds the ratio between suitable area and floor area SAFAR$_n$ was also calculated.

Table 3.3 Solar irradiation thresholds / (kWh/m^{2}a)

Unsuitable	Suitable		
	Reasonbale	Good	Very Good
0-650	651-899	900-1020	> 1020

Since this research was solely focused on PV solar systems, a coverage of 100% on all usable suitable areas (75% of the total surface area) was considered. Calculations on the load coverage, represented by the solar fraction, which is the ratio between the electricity provided by the PV system and the electricity demand of the building, usually on an annual basis, were based on 10 kWh/m^{2}a for common electricity and a guideline value of 30 kWh/m^{2}a for household electricity for new buildings. The results generated from the load coverage for all SAFAR$_n$ studies represent more of a theoretical maximum potential, rather than a realistic scenario, since many aspects of the PV system were not considered, which would affect the outcome. The results generated for the study of the solar energy building assessment tool calculated the hourly load matching based on an existing consumption profile, providing the necessary detail to fully analyse the solar potential for electricity production. For all used input data see Table 3.4.

Table 3.4 List of input data used for both SAFARn study and assessment tool, indicated accordingly

Weather data	Copenhagen, Denmark
Analysis period	

- SAFAR$_n$ - Assessment tool	DIVA: Annual (1 Jan – 31 Dec) Honeybee: Hourly (1 – 8760 hours)
Radiance parameters Grid size Nodes offset	-ab 3, -ad 2048, -as 512, -ar 256, -aa 0.1 0.5x0.5m 0.001m
Reflectances - SAFAR$_n$ - Assessment tool	 building surfaces: 35%; ground: 20% building surfaces: 35%; ground: 20%; PV panels: 10%
Usable surface area	75%
Storey height	3m
PV - SAFAR$_n$ - Assessment tool	 PV coverage: 100%; PV efficiency: 15% PV coverage: 100%; PV efficiency: calculated PV panel: 1 x 1.5m
Common electricity Household electricity (plug load)	10 kWh/m^{2}a 30 kWh/m^{2}a

3.4 SAFAR$_n$

3.4.1 Grasshopper-based script for SAFAR$_n$ simulations

The working process started with the creation of a Grasshopper-based script that was used to perform the solar irradiation simulations. Grasshopper was the backbone of the script, connecting the geometry created in Rhinoceros to the simulation tool DIVA. Furthermore, all visual and numerical results were exported into familiar file formats .csv (Excel) and .jpeg (any image viewer). SAFAR assessment workflow is presented in Figure 3.2.
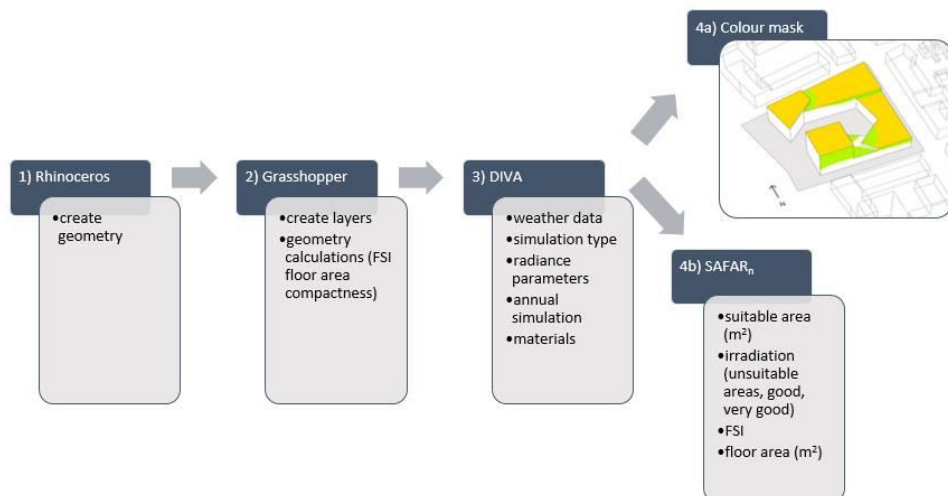
Figure 3.2 SAFAR assessment workflow

1) **Rhinoceros**

To create the models, the process could begin by importing a CAD, a SketchUp file, or they could directly be modelled in Rhinoceros. In this study, the buildings were modelled in Rhinoceros, using meters as a measure unit and dividing each geometry into three layers for the building, the plot and the surroundings. Shading from the surrounding buildings has a great effect on the solar potential, especially in an urban context, therefore, their geometry must be assigned to a layer.

2) **Grasshopper**

- **Geometry layers**: In order for the Grasshopper script to recognize the geometry of 3D models present in Rhinoceros, components that recognize the layer names were activated.

- **Geometry calculations:** After geometry identification, this component analysed the 3D geometry of the building to analyse and provided information on the floor area, FSI of the building, FSI of the surroundings and compactness. Furthermore, the script was able to perform geometry calculations for different envelope surfaces such as flat roof, pitched roof and facades.

3) **DIVA**

After the geometry was set and all related parameters were calculated, materials for the building, the ground and the surroundings, in order to account for shading were set (see Table 3.4). It is also worth to mention that the calculation method for the solar irradiance considers reflections from any surrounding objects or buildings. The next step was to setup an annual solar irradiation simulation by performing an analysis grid of 0.5 x 0.5 m, location, simulation type, analysis period, and Radiance parameters as previously described in Table 3.4.

4) **Export**

When the simulation was finished, the irradiation data was processed and divided between the roof and facade surfaces and SAFARn was calculated. Once this was done a colour mask was assigned corresponding to the pre-determined solar irradiation thresholds:

- White – unsuitable 0-650 kWh/m^{2}a
- Green – reasonable 651-899 kWh/m^{2}a
- Yellow – good 900-999 kWh/m^{2}a
- Red – very good > 1020 kWh/m^{2}a

The final step was to gather all generated results and export them as a .csv file which contains output information about $SAFAR_n$ for different irradiation values on roof and facade,

categorized irradiation values and areas on roof and façade, as well as floor area, FSI and compactness. Additionally, images from four different orientations were exported into a .jpeg file to provide a visual representation of where the suitable and unsuitable areas are on the building. The results were later processed in post-processing software (Excel) in order to calculate the PV potential of the buildings. The PV output was calculated using Equation 3, assuming the PV panels are placed horizontally on the roof and vertically integrated on the façade.

$$PV_{output} = (E.A).\eta_{PV}.\eta_{syst}$$

<div align="right">Equation 3</div>

E – The sum of all radiation values for each suitable surface over the year (kWh/m^{2}a)
A – The net available area for PV (according to the usable surface area of 75%)
η_{PV} – module efficiency (%)
η_{syst} – system efficiency (%)

3.4.2 Hyllie case study

Hyllie (55° 34' N, 12° 58' E), a district in the city of Malmö, is going through a major development with many new planned multi-storey residential and commercial buildings (Hyllie, 2015). Most of the buildings that have been designed in the zoning plan have flat roofs and mainly follow a geometry with inner courtyards. The height of the buildings varies, but only in some cases exceeds 12 floors (see Figure 3.3).
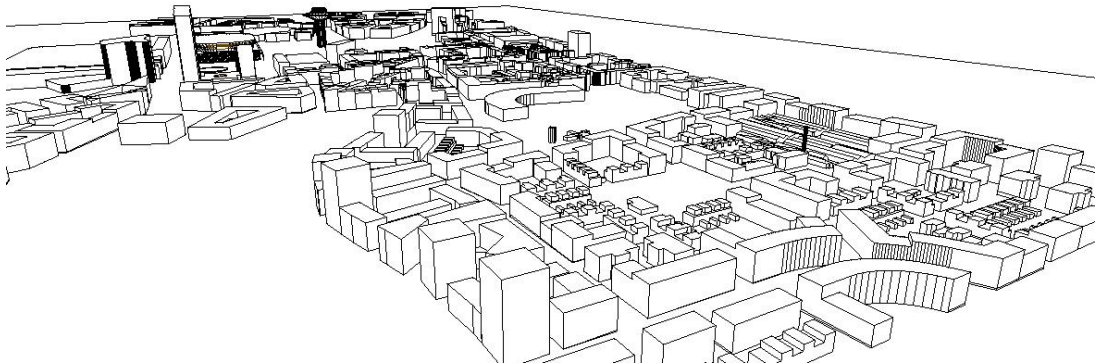
Figure 3.3 Hyllie's planned district

In this section, the focus will be on seven residential buildings, selected from the zoning plan (see Figure 3.4 and Figure 3.5), indicated with their plot names, which had a different surrounding context, varying roof heights and building dimensions.
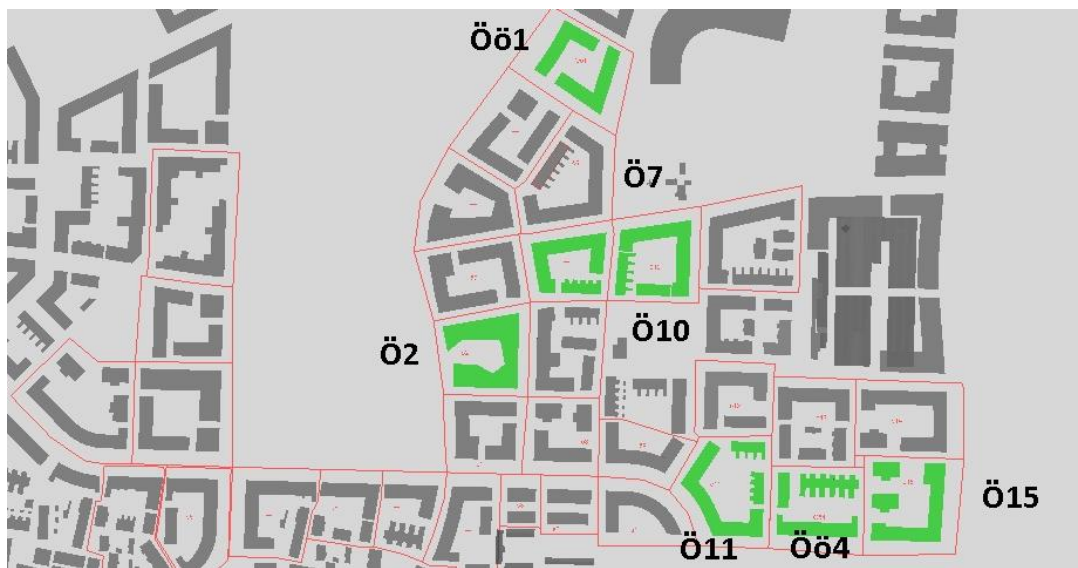
Figure 3.4 Plan view of Hyllie with the selected buildings

Building Ö2 Floor area: 13693 m^2 Surroundings:north and south: buildings with similar geometry; west: open space; east: buildings with slightly lower height	Building Ö7 Floor area: 7840 m^2 Surroundings:all directions: buildings with similar height
Building Ö10 Floor area: 10494 m^2 Surroundings:north and south: open space; west and east: buildings with similar height	Building Ö11 Floor area: 8301 m^2 Surroundings:south: open space; north, east and west: similar height buildings
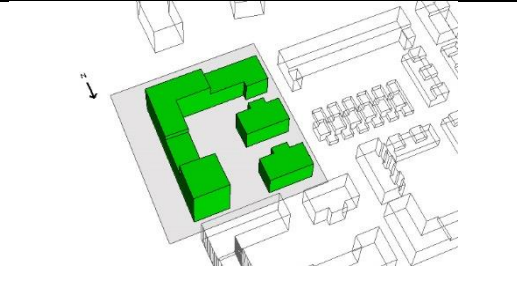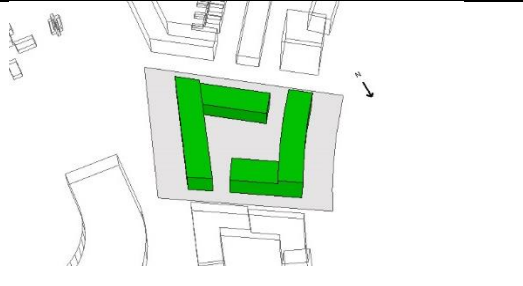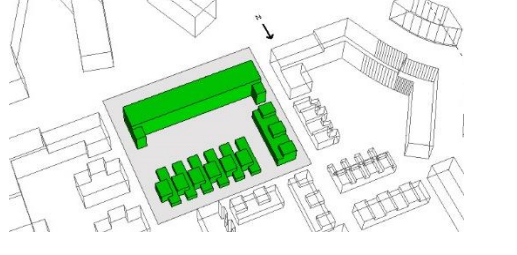
Building Ö15 Floor area: 11507 m^2 Surroundings:east and south: open space (buildings far away); west and north: buildings with similar height	Building Öö1 Floor area: 12099 m^2 Surroundings:south-east and north-west: open space; south-west and north-east: buildings with similar height
	Building Öö4 Floor area: 5322 m^2 Surroundings:south: open space (buildings far away); north, east and west: buildings with similar height

Figure 3.5 3 D view of the seven buildings, Hyllie

Using the Grasshopper-based script for SAFAR$_n$ simulations, each building was examined in terms of suitable area for solar electricity harvesting, expressed by SAFAR$_n$, a visual representation of where the suitable and unsuitable areas are and an annual load coverage calculation for common and household electricity load, based on the PV output. Additionally, the buildings were simulated in two scenarios, with and without surroundings, in order to assess the effect of shading on the building envelope. The buildings' solar potential was also assessed on the basis of their compactness and their density.

3.4.3 The effect of the surroundings

The assessment of how the surrounding context influences the solar potential of a building was applied in a parametric approach, therefore, one theoretical building block that resembles the building typologies described in the Hyllie case study (see Table 3.5) was chosen, due to its convenience in terms of alteration of the parameters. Furthermore, an assessment of the potential load coverage was also assessed on basis of an annual PV production.

Table 3.5 Base case building

Building dimensions / (m)	50 x 50
Roof type	Flat
Floor area /(m^2)	9120
FSI	2.45
Height / (m)	15
Number of floors	5
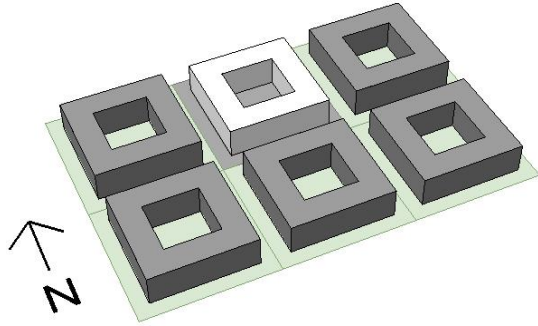
In order to evaluate the effect of shading, the building was first simulated without any surrounding buildings to form a base case to which all result were later compared ("Freerun"). A parametric study was carried out on surrounding's parameters in order to identify a relationship between solar potential, density (openness between buildings and height of the neighbouring buildings) and the effect of different facade materials. The examined building was not altered in any way, however, the FSI of the building changed when the street parameter was modified, due to the reason that the plot area includes half of the surrounding streets.

The parameters of street width and building's height were varied together, and each street width was simulated for all number of floors (see Table 3.6). The chosen street dimensions were based on Larsvall et al. (2010), where four different street types were identified in Malmö, but instead generic values were used. The amount of floors for the surrounding buildings was varied from 1 storey to 13 storeys in an increment of 2 storeys (1 storey has a height of 3m). The reason for that was the assumption that 1 storey variation would show a negligible effect. The maximum height of 13 storeys is not that common for a Swedish urban context, however for the purpose of the case study this aspect was neglected. In this simulation the buildings adjacent to the north side of the building were omitted, since their overshadowing effect on the solar access was negliglible.

Table 3.6 Variables for street width and number of floors

Street width / (m)	10, 15, 20, 30
Number of floors	1,3, 5, 7, 9, 11, 13

Another parameter that was studied looked at the contribution of the indirect solar radiation, reflected from the surrounding buildings. Facade materials with different reflectance values were selected, in order to account for different scenarios such as highly glazed buildings with high reflectance or buildings with dark and absorptive surface (see Table 3.7). In order to fully examine the effect of reflections, buildings on the northern side were added to the model (see Figure 3.6). Furthermore, the simulations for each material were

carried out for building heights based on the ones used for investigation of street width and surrounding buildings' height. It was assumed that the effect of the reflected indirect radiation will be small at heights lower than the examined building, therefore the study looked at surroundings with 5 floors and higher. Additionally, a street width of 15m was selected as common for a context in southern Sweden.

Table 3.7 Facade materials, according to Radiance material library (R=red, G=green, B=blue)

Material	Description	R	G	B	Secularity	Roughness
Default surface	Void plastic	0.35	0.35	0.35	0	0
Metal façade	Void plastic	0.5	0.5	0.5	0.95	0.175
Concrete plaster	Void plastic	0.69	0.71	0.72	0	0
Black colour façade	Void plastic	0.1	0.1	0.1	0	0
Green façade	Void plastic	0.15	0.6	0.2	0	0
Material	Description	R	G	B	Transmittance	Transmissivity
Glazing double pane	Void glass	0.8	0.8	0.8	0.88	0.87
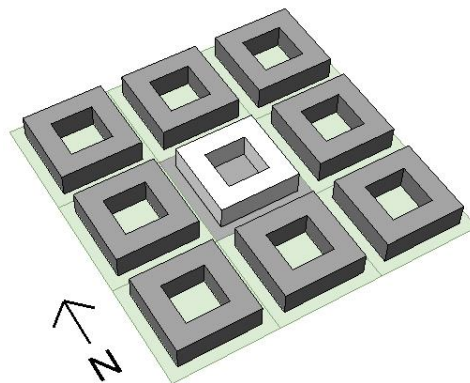
Figure 3.6 Base case building with buildings on the north

3.5   Solar energy building assessment tool

This subchapter explains the workflow of the solar energy assessment tool, together with the decisions behind it. Furthermore, the capabilities of the tool are demonstrated on a building, following a step-by-step approach. In the end, results for the suitable area ($SAFAR_n$), system size and setup, electricity generation and load coverage are demonstrated as output results.

3.5.1 Tool workflow structure

Step 1)   Calculation of SAFAR$_n$

The first step of the workflow was performed in the same way as in the evaluation of seven buildings from the Hyllie case. After an annual solar irradiation simulation was run, a clear picture of the location and the amount of areas suitable for a solar energy system could be identified. At this stage of the process, the design could be either optimized, either carried on with the next step. Within the framework of this study no optimization strategies were implemented.

Step 2)   Setting up of the PV system

The second step of the process was to assign the solar irradiation threshold for suitable areas, which determined the areas for installing the PV system. In order to make the tool more flexible when setting up the system, the geometry of the suitable surfaces was divided into roof and façade. This way a further assessment of each individual surface could be carried out and a different system setup could be assigned, if needed. Based on that information and an input of a PV panel size, the system is placed according to predefined orientation, row spacing and module inclination parameters. Once a system was assigned to a surface, the script generated a system that fits accordingly, based on the above mentioned parameters and was visually presented. Since the panels were introduced to the model, the calculation of solar irradiance took into account the effect of mutual shading. At this stage, based on the set up of the panels, a maximum system size could be determined.

Step 3)   Hourly solar irradiation in Honeybee

In step 3, an hourly solar irradiation simulation was created using the simulation plug-in Honeybee (Radiance/DAYSIM), due to DIVA's current inability to output hourly irradiation values. The initial idea to calculate the irradiation for every single panel for a period of 8760 hours could not be implemented, due to the inability of Grasshopper and the computer to handle such a large amount of values. Therefore, an alternative way was implemented, where the centre point of a middle panel from every row was selected as the one with the lowest irradiation. The reason for this decision was the fact that when the script had determined the suitable areas, overshadowing from the neighbouring buildings had already been considered, so the irradiation on the considered suitable surfaces would result in similar values. It is possible that due to mutual shading for panels oriented towards east or west, the panel with the lowest irradiation, in reality to be different, so the results could slightly overestimate the solar irradiation value.

Before proceeding to the simulation, the PV panels were assigned a material with a reflectance of 10%, in order to account for the absorptive capabilities of the real modules. Additionally, the used Radiance parameters were the same.

Step 4)   Calculation of the PV output

The PV performance is dependent on many factors, but at conceptual stage of a project not much detail about the system is known. However, it is known that the output of the system is strongly dependent on the efficiency losses due to heating up of the module by the incoming solar radiation. Therefore, the temperature dependency of the hourly PV output was implemented into the calculation.

At the beginning, a script made in Grasshopper, using the EnergyPlus simulation engine, was tested for a calculation of the surface temperature, and later implemented into the cell temperature calculation. However, due to geometry problems that the script could not solve, the model did not perform as expected. For this reason, the validated temperature correction method for flat plate PV called Sandia (King et al., 2004) was chosen instead. It is worth to mention that a validated solar energy tool such as System Advisor Model (SAM) has this method integrated in one of its modelling modes (NREL, 2015). This approach poses some limitations of the method, since at an early design stage such a level of detailed information is not known.

Before calculating the cell temperature, the temperature correction algorithm was used to calculate the temperature at the back of the module (T_{back}), based on the incidence radiation ($E_{incident}$) as well as a and b coefficients that are empirically-determined coefficients based on the type of module structure and mounting (NREL, 2015). Additionally, the calculation considered the hourly wind speed (V_{wind}) and the hourly ambient temperature ($T_{ambient}$) taken from the weather data (see Equation 4). Taking wind into account would result in a more accurate estimation of the cell temperatures, especially in southern Sweden, where the average annual wind speed is 5.5-6.5 m/s (Bergström & Söderberg, 2008). Afterwards, the cell temperature (T_{cell}) was calculated based on the modules' back temperature (T_{back}), the incident radiation ($E_{incident}$), the reference incident radiation (E_0), which is 1000 W/m^2, and the temperature difference (dT) between the cell and the module back temperature, which was also a predefined value based on the module structure and the mounting (see Equation 5).

$$T_{back} = E_{incident} \cdot e^{a+b*V_{wind}} + T_{ambient}$$

<div align="right">Equation 4</div>

$$T_{cell} = T_{back} + \frac{E_{inciden}}{E_0} \cdot dT$$

<div align="right">Equation 5</div>

In order to calculate the output of the PV system, the next step of the calculation was to calculate the maximum power of the module (P_{mp}), after the temperature correction, which is also based on the module model. The calculation takes into account the maximum power of the module at ideal conditions (P_{mp0}), the temperature correction factor (γ), based on the cell type, the temperature of the cell and the reference temperature (T_{ref}), which is the temperature manufacturers normally test the modules at Standard Test Conditions (STC) (see

Equation 6). Further on the hourly efficiency was calculated using the P_{mp}, the reference incident radiation (E_0) and the area of one panel (see Equation 7).

$$P_{mp} = P_{mp0} \cdot [1 + \gamma \cdot (T_{cell} - T_{ref})]$$

Equation 6

$$\eta_{PV} = \frac{P_{mp}}{E_0 \cdot A_{PV}}$$

Equation 7

Based on the result, the calculation of the electricity output of a panels (PV_{output}) was calculated by the hourly irradiation on the panels in kWh (E), the hourly efficiency of the module (η_{PV}), a fixed value of 10% for additional losses of the system (η_{syst}) and the area per panel (A_{PV}) (see Equation 8).

$$PV_{output} = E \cdot \eta_{PV} \cdot \eta_{syst} \cdot A_{PV}$$

Equation 8
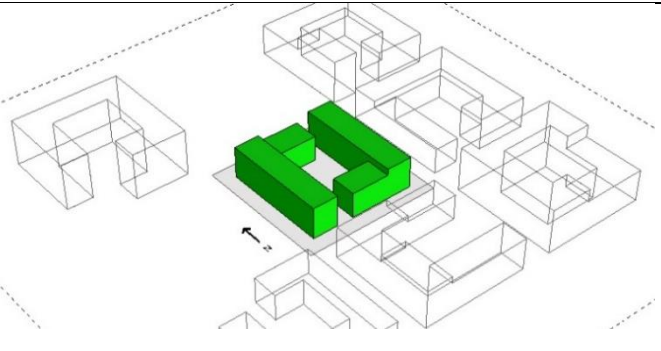
Step 5)   Load matching

In step five, the system output for an annual and hourly production was processed and plotted against an electricity consumption profile for the common and plug electricity loads. The results for an annual solar fraction and more detailed results of the hourly load coverage (self-consumed electricity) were obtained for every suitable surface of the building. The next logical step of process could lead to estimation of the financial parameters of the PV system, however in this study this was not implemented.

3.5.2 Demonstrating the tool

In order to demonstrate the methodology described above, the assessment tool was tested in a theoretical urban context, where the solar potential of a building block (see Table 3.8), the electricity production, and the load coverage on an annual and hourly basis were evaluated. To validate the results a comparison to the solar energy software System Advisor Model (SAM) was made.

Table 3.8 Description of the examined building

Floor area / (m^2)	6168
Roof type	Flat
Height / (m)	12-15
Number of storeys	4-5
Orientation	N-S
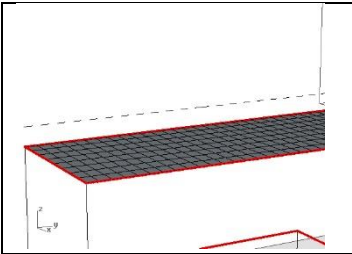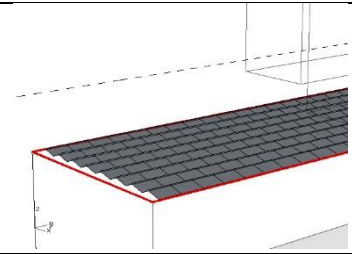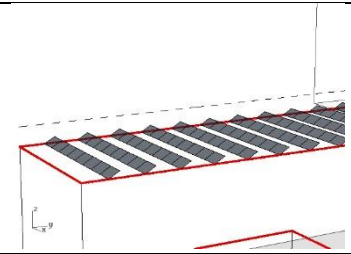
The analysis of the energy production was made on the basis of three different PV system setups, for each of the roof surfaces indicated as suitable (the difference between placing a system on roof areas with irradiation higher than 650 kWh/m^{2}a or 800 kWh/m^{2}a was not included in the study as the difference of the outcome for this building was too small). This was done in order to demonstrate the capabilities of the tool to treat different types of system options. The systems' position on the roof was based on orientation, inclination and row spacing between the panels. These setups aimed at demonstrating different scenarios, such as a systems setup for maximum system output, maximum output per panel and a system with a low inclination towards east and west (see Table 3.9). The system for maximum output (setup 1), is theoretical, since for such a large roof area, an installation like that needs a distance in-between the panels for inspection and maintenance. Moreover, problems with snow and rain run-off would occur.

Additionally, for systems placed on the suitable facade a vertical placement along the surface was implemented, as they were building integrated.

Table 3.9 PV system setups on the roof (note: south is indicated as 0° azimuth)

	Inclination / (°)	Row spacing / (m)	Azimuth / (°)
Setup 1	0	0	0
Setup 2	15	0.5	-90/+90
Setup 3	30	2	0

Table 3.10 PV system setups on the roof

Setup 1	Setup 2	Setup 3

In order to perform an hourly load match calculation, an electricity consumption profile for an apartment block was obtained from Öresundskraft, an energy company provider in Sweden. The data for the common electricity were based on a building heated by district heating, therefore the only additional electricity load in the building came from the household electricity. The obtained data was needed to establish the hourly consumption profile and adapt it to the buildings assumed electricity consumption (floor area multiplied by the chosen value for common electricity load of 10 kWh/m²a) (see Figure 3.7). Since no data could be obtained for the plug electricity load (household electricity), the same process was applied to create a consumption profile for the guideline value of 30 kWh/m²a, used by SVEBY (2012).
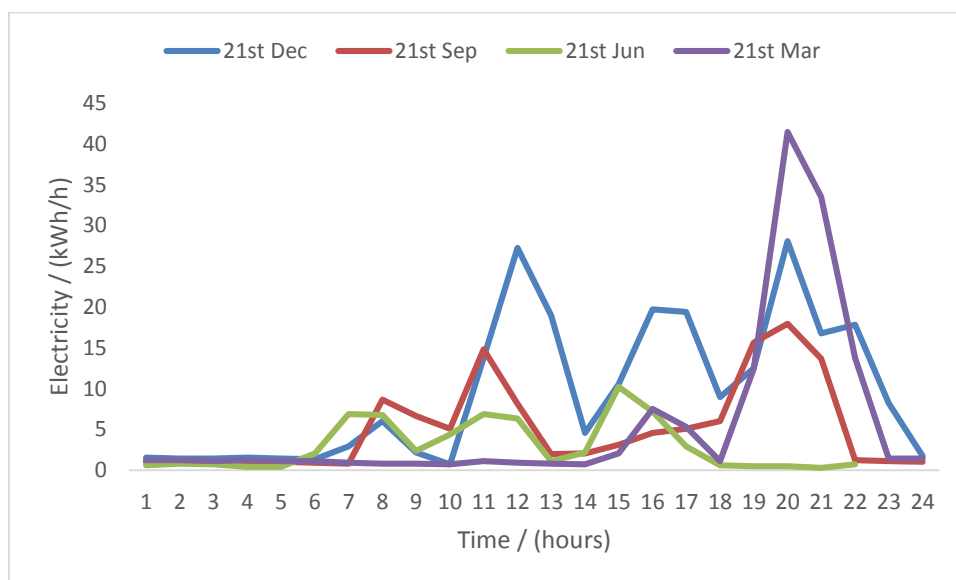
Figure 3.7 Daily electricity common load

The tool used a temperature correction factor for performing the PV output simulations, as it was described earlier. In order to proceed with the simulation, the cell type, the module structure and the mounting had to be selected. It was assumed that facade systems would normally be building-integrated (BIPV), as for the roof system it was assumed that in order to avoid overheating of the panel, there will always be an air flow between the roof surface and the PV panels. As for the cell type, silicon was chosen since it is the most common on the market (IEA-PVPS, 2014). The chosen input parameters can be seen in Table 3.11.

Table 3.11 Input data

Weather data	Copenhagen, Denmark
Analysis period	Honeybee: Hourly (1 – 8760 hours)
Radiance parameters	-ab 3, -ad 2048, -as 512, -ar 256, -aa 0.1
Grid size	0.5x0.5m
Nodes offset	0.001m
Reflectances	building surfaces:35%; ground: 20%; PV panels: 10%

Usable surface area	75%
Storey height	3m
PV	PV coverage: 100% (for 75% usable surface area)
PV panel size	1 x 1.5m
Module Structure & Mounting Roof: Façade:	Glass/Cell/Polymer Sheet Open Rack Glass/Cell/Polymer Sheet Insulated Back
Roof: a-coefficient b-coefficient dT	-3.56 -0.0750 3 °C
Façade: a-coefficient b-coefficient dT	-2.81 -0.0471 0 °C
Pmp0	200 Wp
Maximum Power Temperature Coefficient (%/°C)	Cell type: Silicon -0.49
Common electricity Household electricity (plug load)	10 kWh/m²a 30 kWh/m²a

The validation of the obtained results compared to System Advisor Model (SAM) was based on the three system setups considered in this study, with the corresponding system size (in kWp). In SAM, the Simple Efficiency Module Model (NREL, 2015) was used, which uses a fixed module efficiency of 15% and the Sandia temperature correction method for flat plate PV modules (King et al., 2004), also used in this research.

4 Results and Discussion

4.1 SAFAR$_n$

The following section presents an evaluation of two studies on solar potential and their subsequent PV potential. The first study investigated seven building designs from Hyllie area, whilst the second study analysed how different surrounding contexts influence the solar potential of a theoretical buildings block. The output was determined by the solar potential metric SAFAR$_n$ and the area measured in square meters and presented using graphs and 3D images indicating the suitable and unsuitable areas of the building. Furthermore, the calculations were based on annual solar irradiation simulations, which lead to a calculation of the potential PV output and annual solar fraction.

4.1.1 Hyllie case

SAFAR$_n$ solar potential metric was tested on seven cases located in Hyllie, Malmö and assessment of the relationship between solar potential, building form and density was done.

Figure 4.1 visualises which areas of the buildings are suitable for solar panels, as well as the contribution of shading from the neighbouring buildings. For all buildings, the roofs affected by self-shading and the south-facing façades are indicated as suitable with irradiation over 650 kWh/m^{2}a, and over 800 kWh/m^{2}a for roofs which are generally not shaded. When the surroundings are omitted, the south facades are fully available, while the east and west facades are still result irradiation values under 650 kWh/m^{2}a, therefore, indicated as unsuitable.

Ö2 with surroudings   Ö2 without surroundings

< 650 kWh/m^{2}a	651 – 899 kWh/m^{2}a	900 – 1020 kWh/m^{2}a	> 1020 kWh/m^{2}a
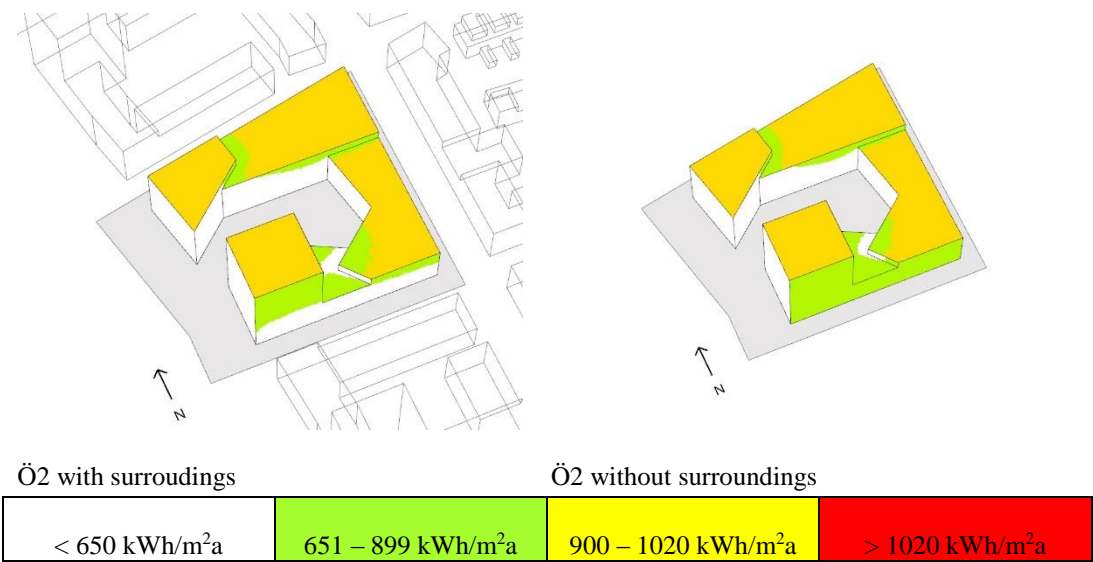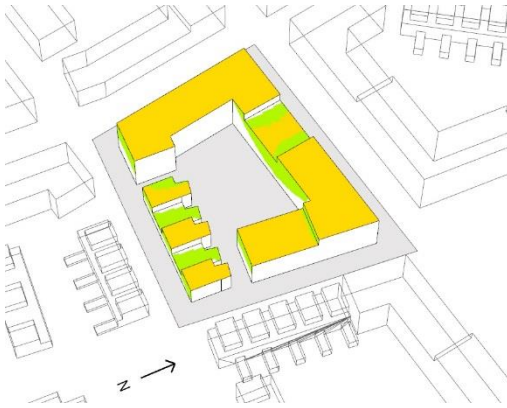
Ö7 with surroudings
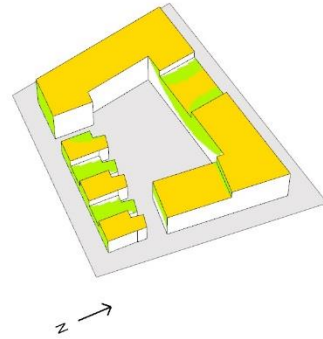
Ö7 without surroundings

Ö10 with surroudings
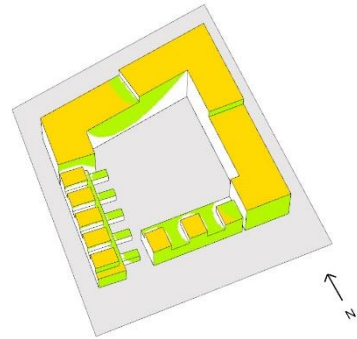
Ö10 without surroundings
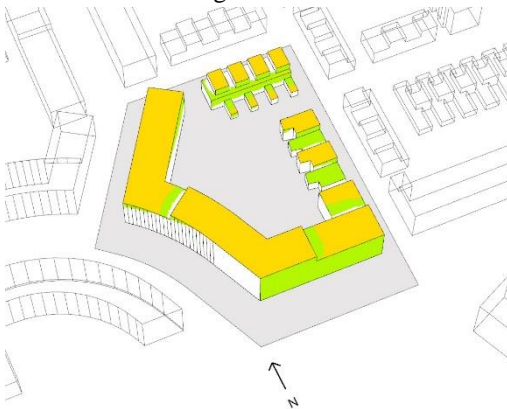
Ö11 with surroudings

Ö11 without surroundings

Ö15 with surroudings   Ö15 without surroundings

Öö1 with surroudings   Öö1 without surroundings
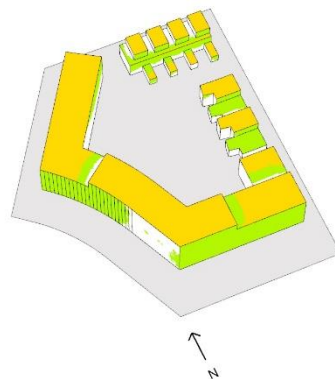
Öö4 with surroudings   Öö4 without surroundings
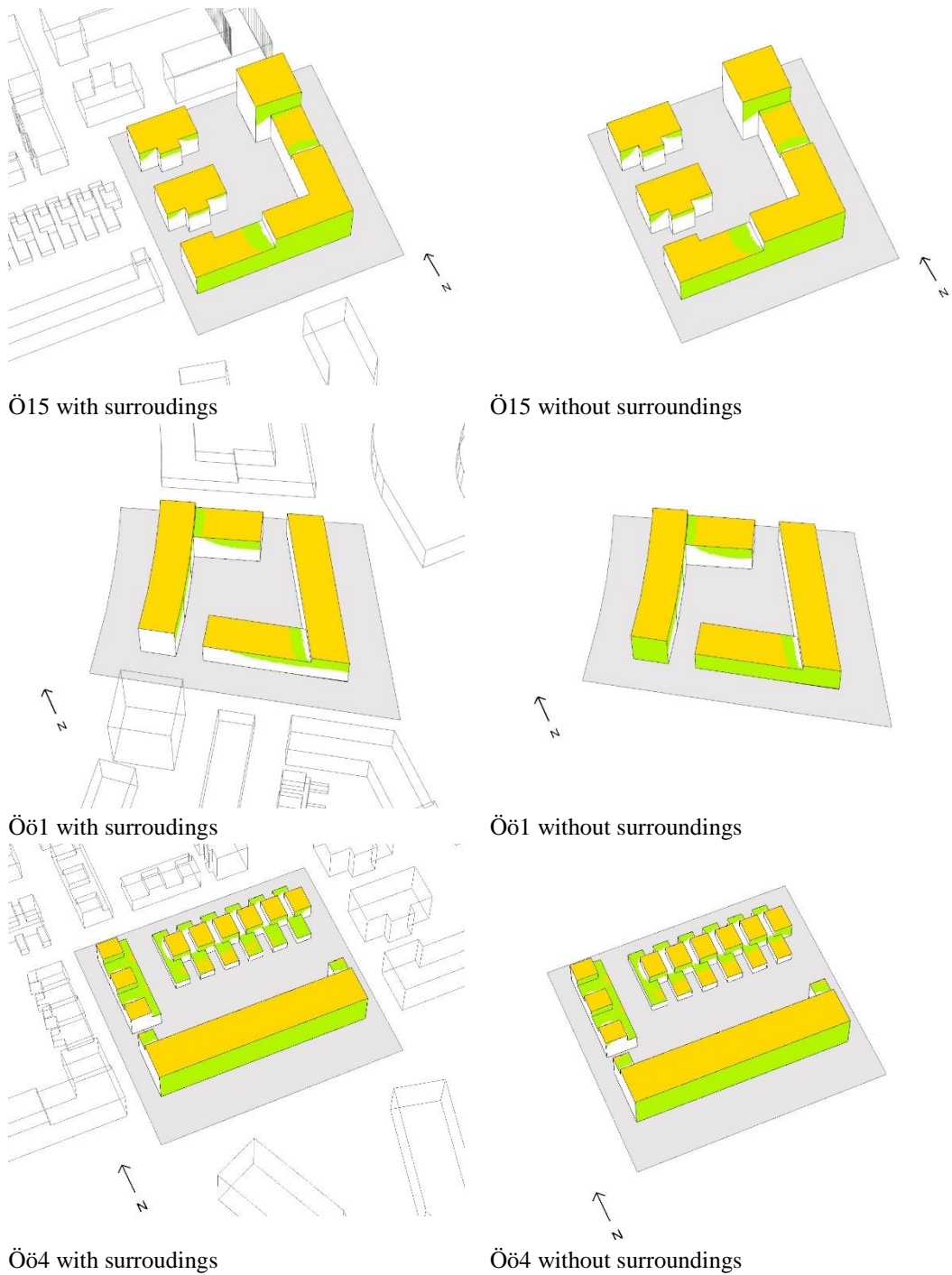
Figure 4.1 Visual representation on the suitable areas of all seven buildings

Figure 4.2 represents the results for $SAFAR_{650}$ for all buildings, with and without the surrounding context. The solar potential calculations for $SAFAR_{650}$ indicate the suitable area to floor area ratio for each building. Each building has a different surrounding context,

43

therefore the impact of shading differs. Since most of the buildings in the study have similar heights, except for building Ö2, the roof potential is only affected by self-shading and not from the surroundings. Building Ö2 has one roof surface that is much higher than the rest, but it still only affects its own adjacent roof (see Figure 4.2). However, for buildings with large facades facing south or south-west (Ö2, Ö11 and Öö1), the impact of the surrounding context has a significant effect on the solar access (see Table 4.1). For buildings with an open space in front of their suitable facade surface, the difference is either very small or non-existent (Ö7, Ö10, Ö15 and Öö4).
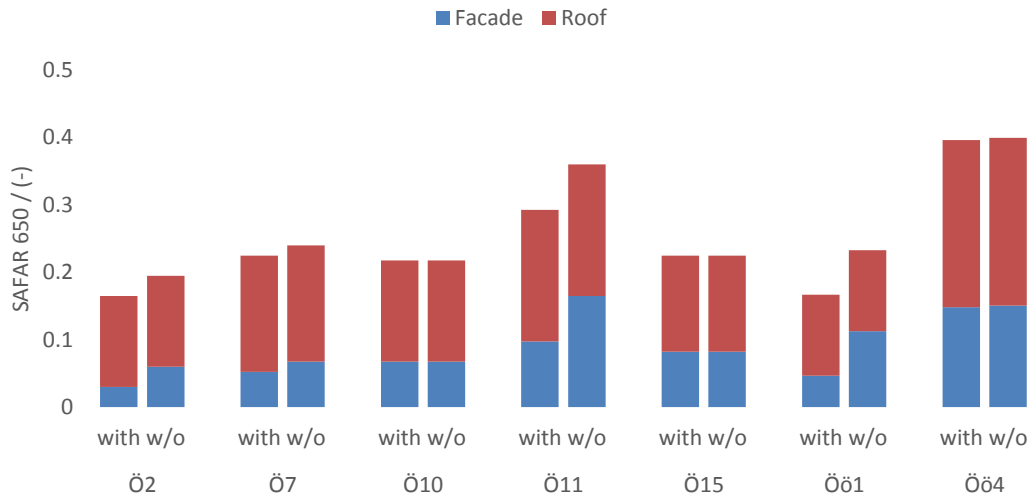
Figure 4.2 SAFAR650 for seven buildings, with and without (w/o) surroundings.

Table 4.1 Percentage difference between a case with surroundings and a case without surroundings.

Buildings	Ö2	Ö7	Ö10	Ö11	Ö15	Öö1	Öö4
Losses	15%	6%	0%	19%	0%	28%	1%

The results demonstrated that in the examined contexts, the surroundings have the greatest effect on the facades and not on the roof. In order to be able to compare all buildings solely based on their building form, the following calculation presents the buildings without their surrounding context. Figure 4.3 and Figure 4.4 demonstrate the relationship between $SAFAR_{650}$ and building density (FSI_{plot}) as well as relationship between $SAFAR_{650}$ and the compactness ratio.

The calculation results indicate that the buildings with a lower building density (Öö4 and Ö11) and higher compactness ratio (meaning the buildings are less compact) have better SAFAR values (see Figure 4.3 & Figure 4.4). It is also evident that the building density and the compactness are contradictory metrics. The results suggests that buildings with more envelope area per square meter of floor area achieve a higher SAFAR, leading to a less compact building form.
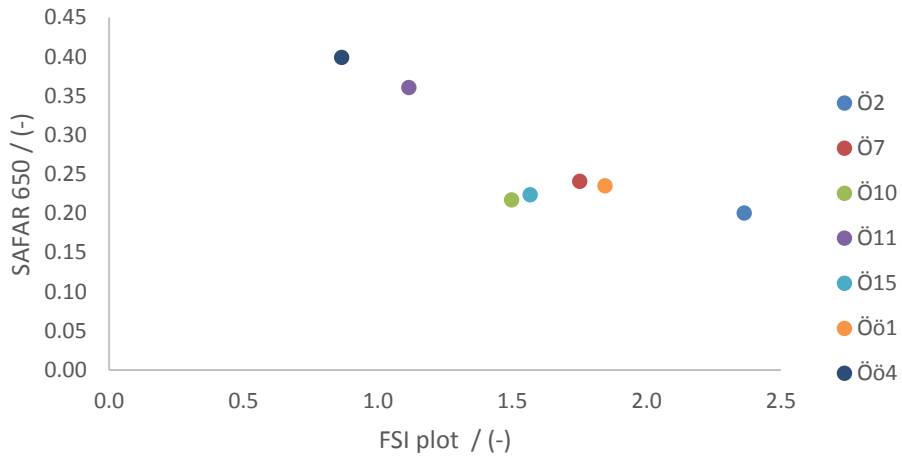
Figure 4.3 SAFAR 650 for the roof surfaces versus FSI plot
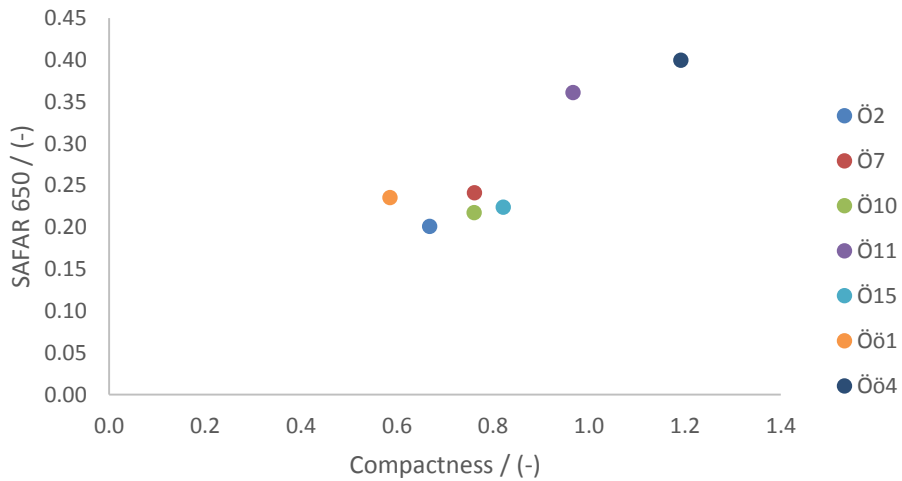
Figure 4.4 SAFAR 650 for the roof surfaces versus Compactness

In Figure 4.5, the reduction in suitable area for each building, based on different irradiation values on the building's surfaces, is presented. It is evident that the amount of suitable area for each building reduces with the increase of the solar irradiation threshold. Irradiation values of 800 and 900 kWh/m^2a are available on unshaded roofs, confirming the overall much higher solar potential of the roof surfaces.
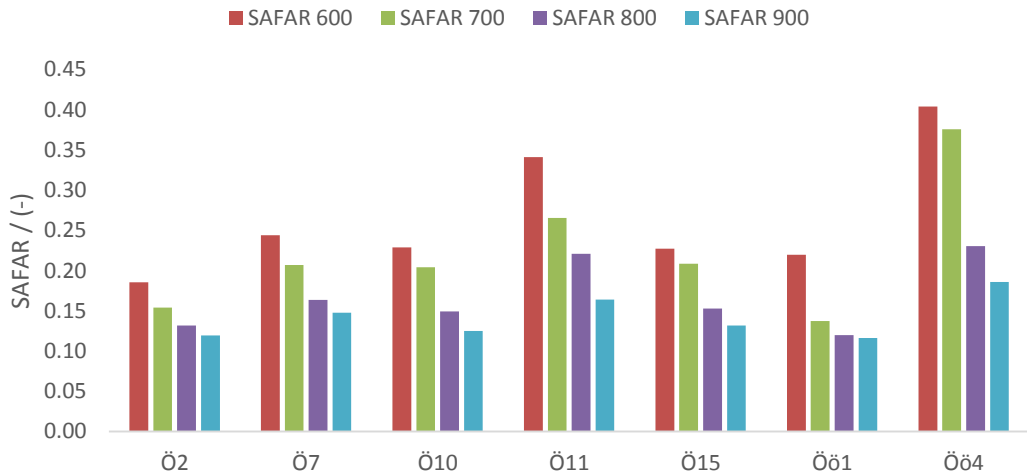
Figure 4.5 The reduction of suitable area with increasing irradiation threshold.

In order to get a better understanding of what the solar potential means in terms of PV output potential, Figure 4.6 shows the annual solar fraction for both common and plug loads for each building. The NZEB represents 100% balance between electricity consumption and electricity production. The results suggest that all buildings have the theoretical capability of covering the electricity for common load. Assuming that all usable area (75%) on the facade can be utilized, buildings Öö4 and Ö11 also have the potential to cover the plug loads, due to their lack of surrounding buildings on the south that affect the irradiation.
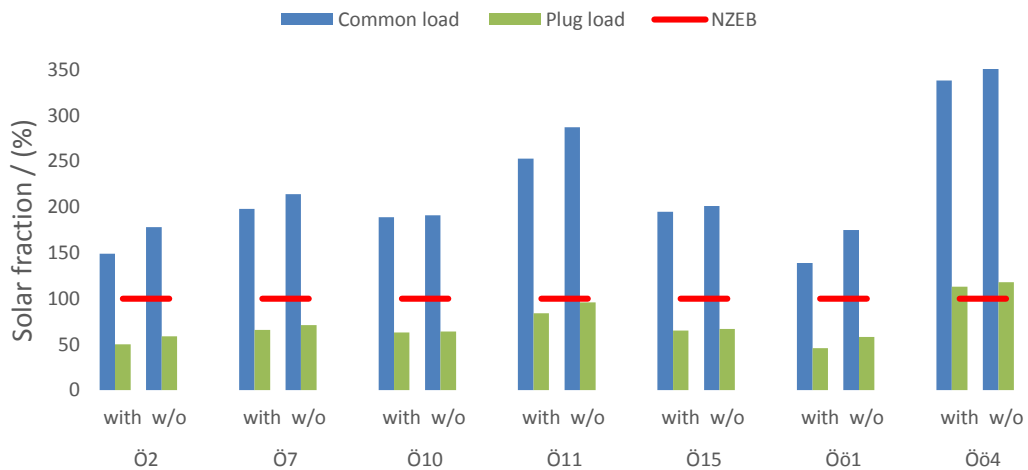
Figure 4.6 Annual solar fraction for common and plug electricity load

The findings of this study part suggest that buildings located in high latitudes (like in southern Sweden, Skåne region), according to the defined irradiation thresholds, are only able to utilize their roof surfaces and south-facing facades or facades with an azimuth angle close to the absolute south, despite the absence of surroundings. This could be explained by the low solar angles for such a latitude and lower direct irradiation values on vertical surfaces in

general. Due to the low solar angles, the effect of shadowing from the surroundings greatly affects the solar potential (SAFAR) of the south facades and limits the building from utilizing these areas. However, in a city context, the likelihood of having no surrounding buildings is very low. The roofs on the other hand, were barely affected by self-shading and returned the highest solar potential.

Apart from the effect of the neighbouring buildings, the building density and compactness proved to be a determining factor of the buildings SAFAR. Due to more available envelope area per square meter of floor area, buildings with lower compactness ratio and higher building density result in a lower SAFAR. This finding was also confirmed by Kanters & Wall (2014), who found that higher density buildings have a reduced solar potential.

In terms of solar fraction, all buildings in theory managed to achieve a solar fraction higher than 100% for the common load on an annual basis. The results could be explained by the insignificant shading of the roofs and the large PV coverage which allow for a large portion of electricity generation. A source of error of these results compared to the reality can be the simplified calculation, assuming that all suitable surfaces are covered with PV panels placed along these surfaces, which in reality is hardly possible for such a large scale buildings.

4.1.2   Surroundings

This section of the research presents the examination of a 5-storey theoretical building typology's solar potential and PV output potential, based on a parametric study on street width, neighbouring buildings' height, and different facade materials. "Freerun" case represents a case without any surrounding buildings, which indicates the maximum SAFAR that the building can achieve and serves as a base for illustrating the contribution of overshadowing.

Street width and different heights

Figure 4.7 shows the relationship between SAFAR, for a threshold of 650 kWh/m^{2}a (considered to be suitable for all building surfaces), and the density of the surroundings, expressed by buildings with a variable height within four types of street widths. The results indicate a linear decline of SAFAR, as the density of the surroundings increases. This effect can clearly be seen starting from a FSI equal to 0 ("Freerun" case) until the FSI reaches 2.5 (same as the examined building). This change is a consequence of overshadowing of the facade of the examined building, which leads to a significant reduction of its suitable area (see also Figure 4.8). For density values between 2.5 and 5, the street width has almost no effect on SAFAR, since the facade becomes unavailable and the roof still receives an amount of irradiation higher than 650 kWh/m^{2}a. The graph also reveals that in terms of solar potential, larger street dimensions allow for higher surroundings.
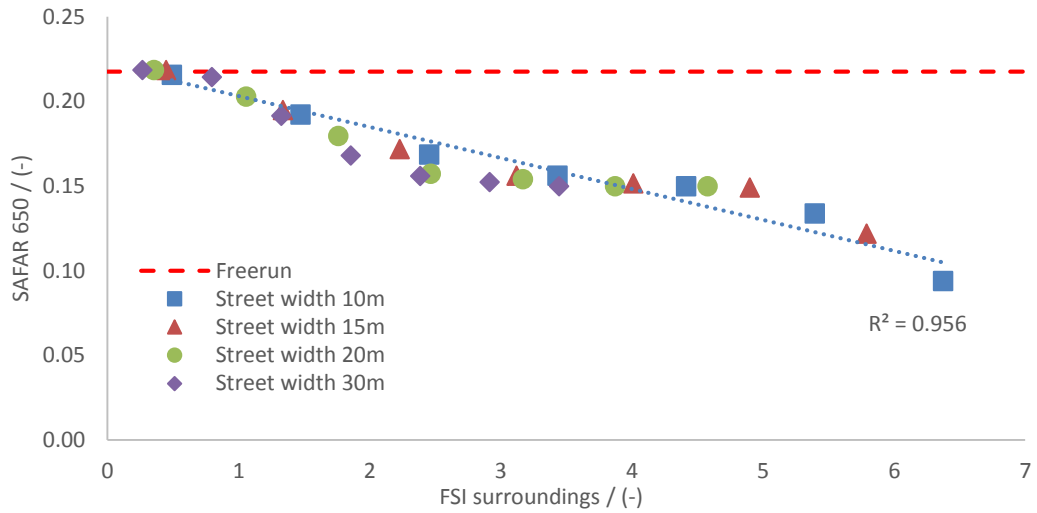
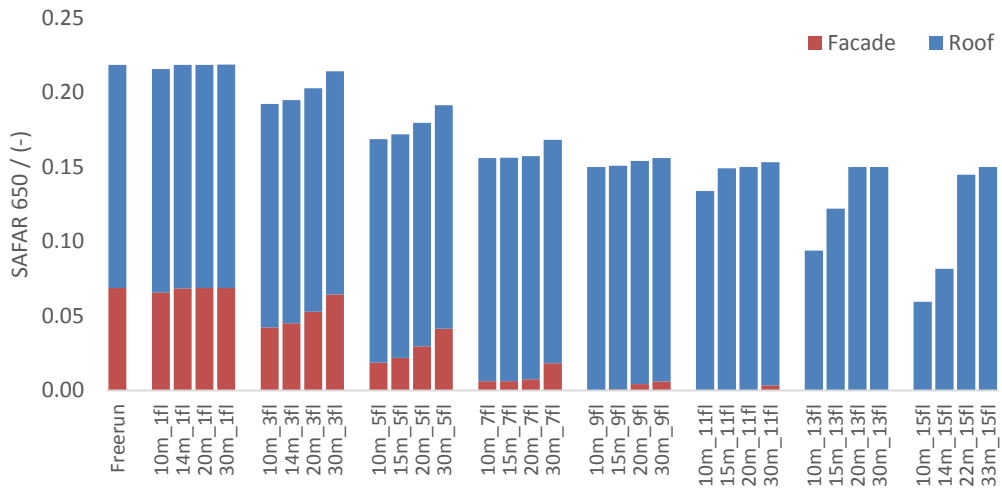Figure 4.7 SAFAR 650 versus FSI surroundings

Figure 4.8 SAFAR 650 for facade and roof, expressed for each building height and street width

Figure 4.8 and Figure 4.9 illustrate how the solar potential is distributed between the facade and the roof surfaces. $SAFAR_{650}$ and the amount of area (m^2) is compared for every building height variation (expressed in number of floors, where 1 floor has a ceiling height of 3m) at a different street width scenario.

Considering $SAFAR_{650}$ (Figure 4.8), the results show that the facade, as expected, performs best when there are no buildings around. As the height of surroundings increases up to 7 storeys, the facade still has a small useful area for PV installation at the top (see Figure 4.9), for all street width parameters. For surroundings higher than 7 floors, for streets of 10m and 15m, the facade becomes unsuitable. For streets of 20m and 30m, $SAFAR_{650}$ is barely present. On the other hand, the roof surface clearly demonstrates more favourable results,

48

where its suitable area is barely affected for heights up to 7 floors, for all street widths. The amount of useful roof area is more significantly affected when the height is increased to 13 floors, for street dimensions of 10m and 15m.

However, as seen from Figure 4.9, if the solar irradiation threshold for roofs is 800 kWh/m^{2}a instead, then the suitable area for street widths of 10m and 15m is greatly affected for heights above 7 floors. For larger street dimensions, the effect is demonstrated for heights above 9 floors.
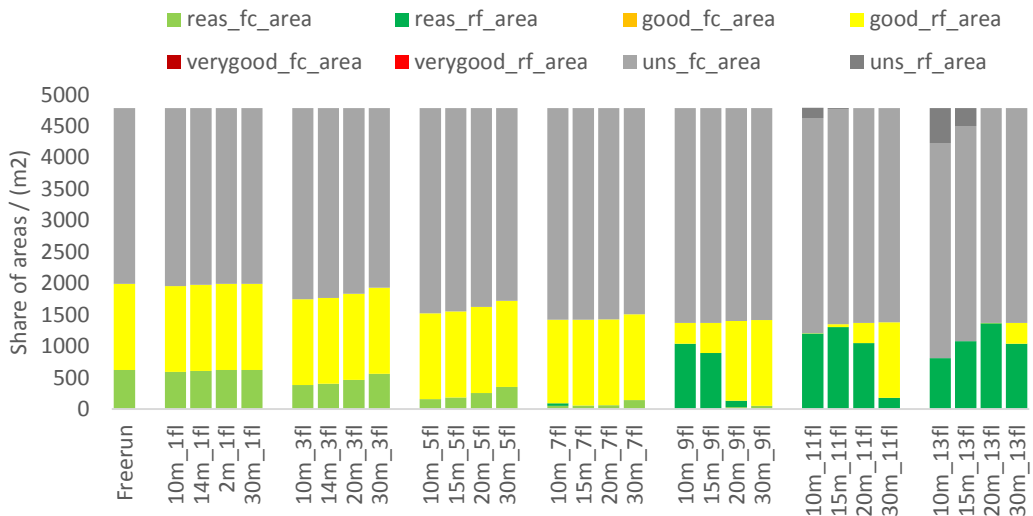
Figure 4.9 Unsuitable, reasonable, good and very good areas, according to solar irradiation thresholds.

Figure 4.10 shows a visual representation example of how the height of neighbouring buildings can affect the solar access and subsequently the amount of suitable area on the southern facade and, with greater heights, the roof of the examined building. The images illustrate the areas that should be considered for an installation of a PV system. The rest of the street width parameters can be seen in Appendix B.

"Freerun"   Street width 15m, 1 floor height
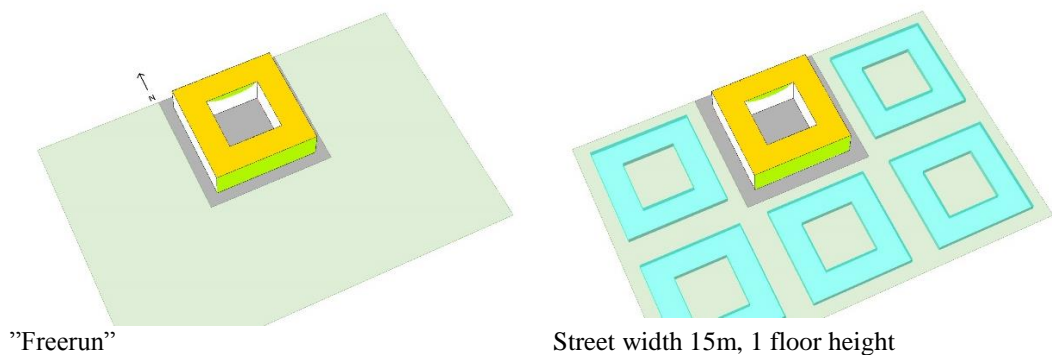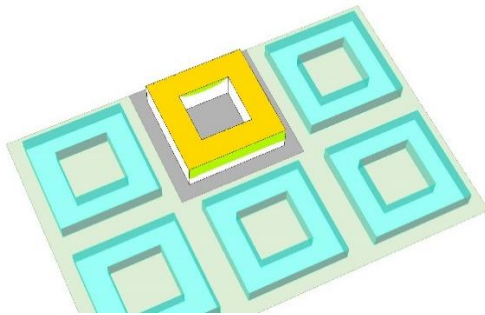
Street width 15m, 3 floors height   Street width 15m, 5 floors height
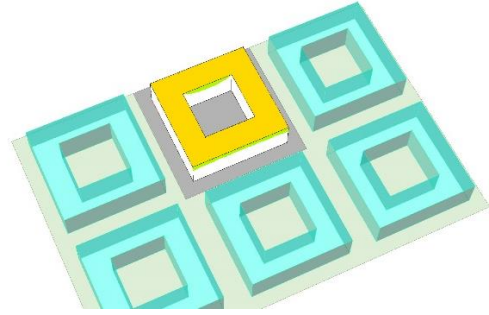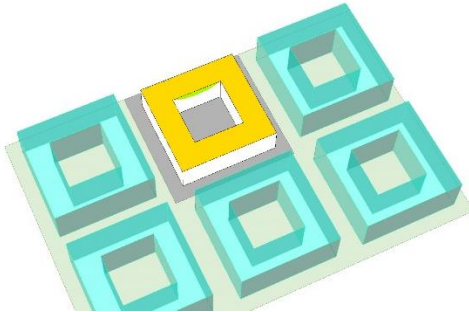
Street width 15m, 7 floors height   Street width 15m, 9 floors height
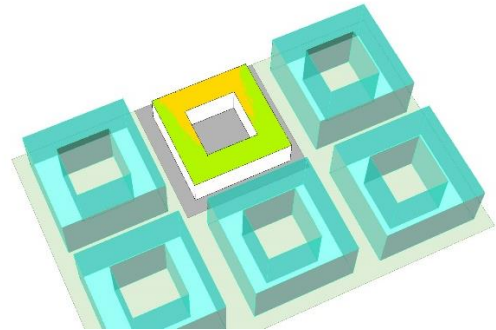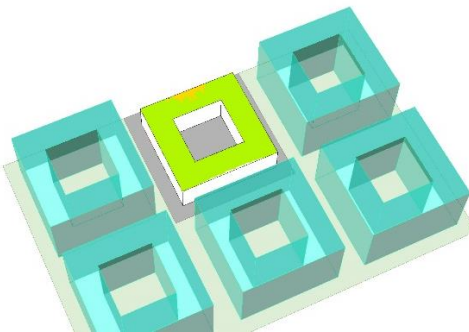
Street width 15m, 11 floors height   Street width 15m, 13 floors height
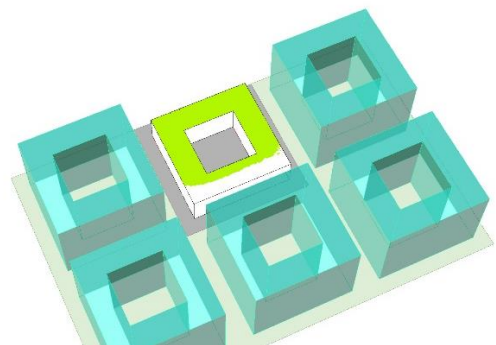
< 650 kWh/m^{2}a	$651 - 899$ kWh/m^{2}a	$900 - 1020$ kWh/m^{2}a	> 1020 kWh/m^{2}a

Figure 4.10 Suitable area for a street width of 15 m

Figure 4.11 shows the maximum potential of the annual solar fraction between the production and the common and plug loads. The results reveal a large difference when adding more floors to the surrounding context, which was not apparent from the results for SAFAR and the distribution of areas. Every step with additional floors on the surrounding context results in 10-20% reduction of the annual coverage and even 30% for 13 floors (examined building has 5 floors), for a street width of 10m. The larger street widths perform better, with all buildings being able to cover the common load of the building. Theoretically, all buildings up to heights of 9 floor appear to be able to cover the common electricity demand. Plug loads however, seem to be difficult to achieve.
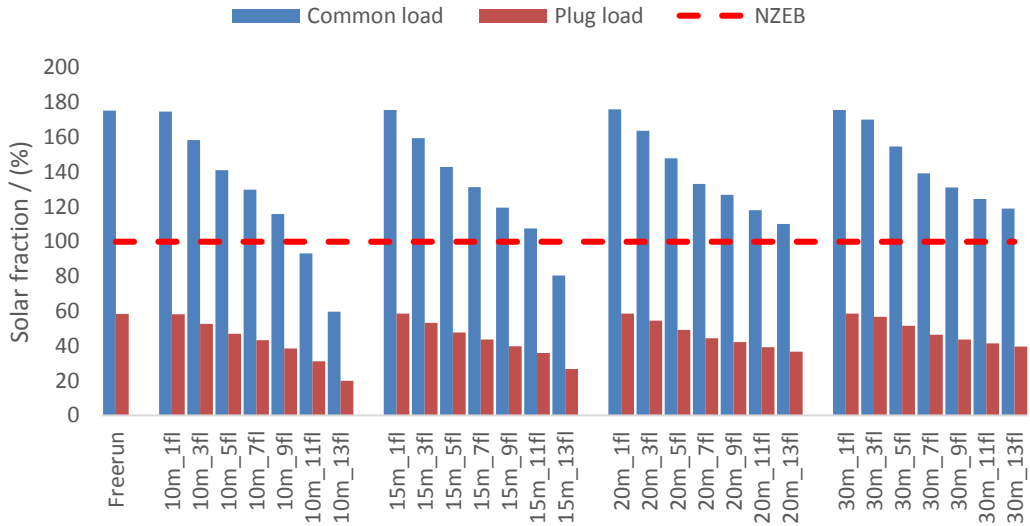
Figure 4.11 Solar fraction for different street width and building heights for SAFAR$_{650}$

As it is shown in the Figure 4.12, if the irradiation threshold for roofs is considered to be $800\,kWh/m^2a$, the results for the solar fraction indicate a large reduction in the PV potential for neighbouring buildings of 7 floors for 10m and 15m street width. For larger street dimensions, a height of 9 floors appears to be the limit in covering the annual common load.
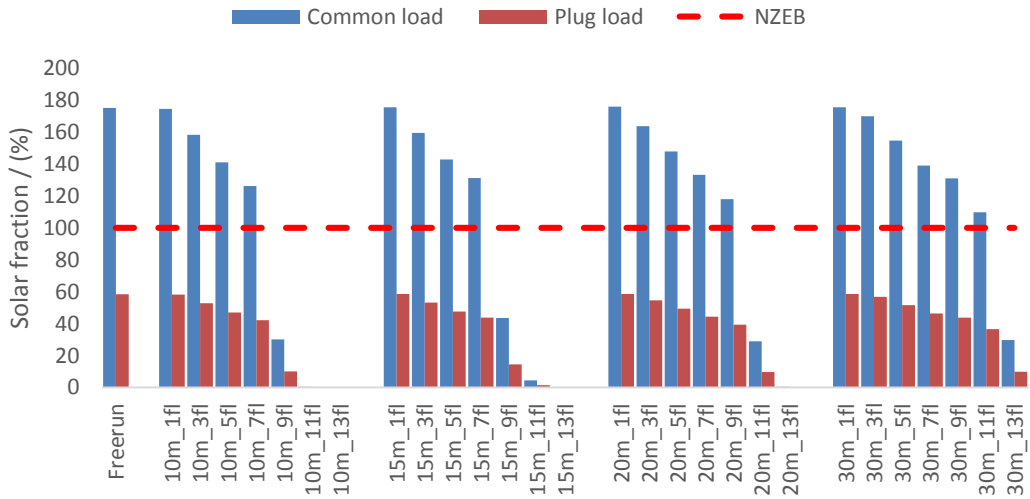

Figure 4.12 Solar fraction for different street width and building heights for SAFAR$_{800}$

What is evident from the results is that larger street width allows for greater surrounding building heights, due to a reduced obstruction angle. However, this requires more land use as well, which raises other issues on an urban level. When considering the facade surface the effect of the street width is more evident. The results indicated the facades are still suitable up to the point when the height of the surrounds is the same as the examined building, for street width of 10m and 15m. For larger street dimensions, the height is increased with two

51

more floors. As the roof surfaces, if the threshold of 650 kWh/m²a is considered suitable, then street width barely matters (except for 10m) for surrounding heights below 11floors (examined building has 5 floors). However, when a solar irradiation threshold for the roof is considered 800 kWh/m²a instead then smaller street dimensions (10m and 15m) the suitable areas and potential solar fraction are extremely reduced when the building are 2 floors higher than the examined building. For larger street widths the height could be increased with 4-6 floors. Overall, a significant difference in the suitable areas was identified between $SAFAR_{650}$ and $SAFAR_{800}$ within different surrounding contexts.

Materials

Figure 4.13 and Figure 4.14 present the results of $SAFAR_{650}$ for different facade materials, based on a fixed street width of 15m and number of floors from 5 to 13. The results of $SAFAR_{650}$ for the facade indicate almost a negligible change from their base cases. The concrete plaster and glazed façades have a slight effect on the solar potential for surroundings' height of 5 and 9 floors. The roof shows an identical scenario, but for buildings with 13 floors, the facade materials behave differently. The black absorptive facade and the green facade reduce their solar potential with 0.01, while the glazed, metal and concrete plaster facades show a slight increase of 0.01-0.02.

However, as shown on Figure 4.14, these changes in fact are more visible on an irradiation and area level. The results show that for buildings with 9 floors, the glazed facade increases the irradiation to the higher threshold of 800 kWh/m²a, which leads to an area of approximately 750 m² with a higher irradiation levels. For the other materials the results vary approximately between +250m² and -250m².
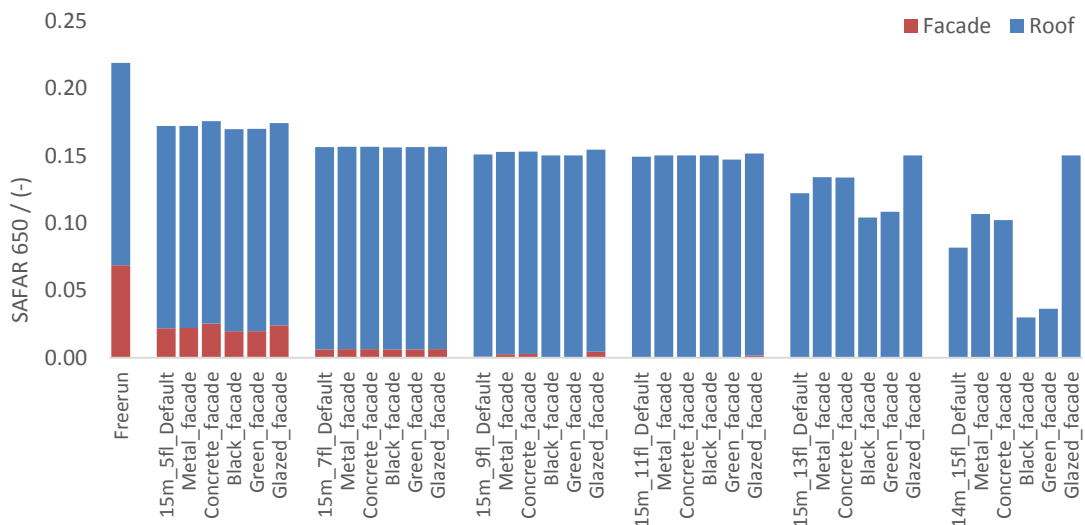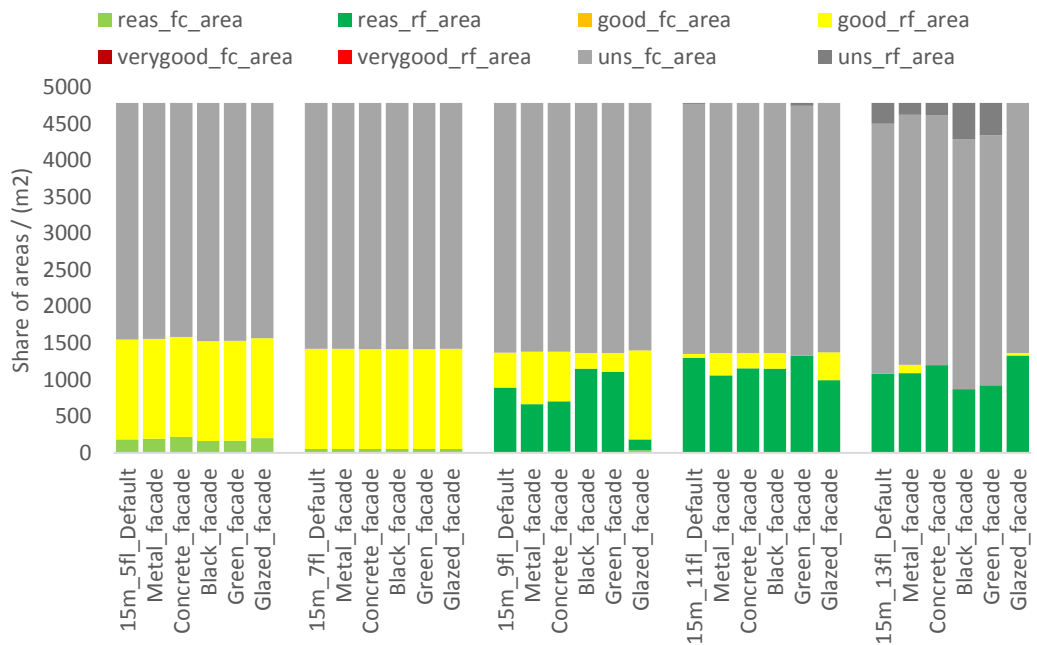

Figure 4.13 SAFAR 650 for different facade materials

Figure 4.14 Area distribution according to unsuitable, reasonable, good and very good classification

Figure 4.15 provides results about the solar fraction for the study of different facade materials. The results show that facade materials with higher reflectance affect the potential of the examined building more noticeable for higher building heights. As observed before the reflective surfaces increase the potential of the examined building by redirecting solar radiation on its surface.
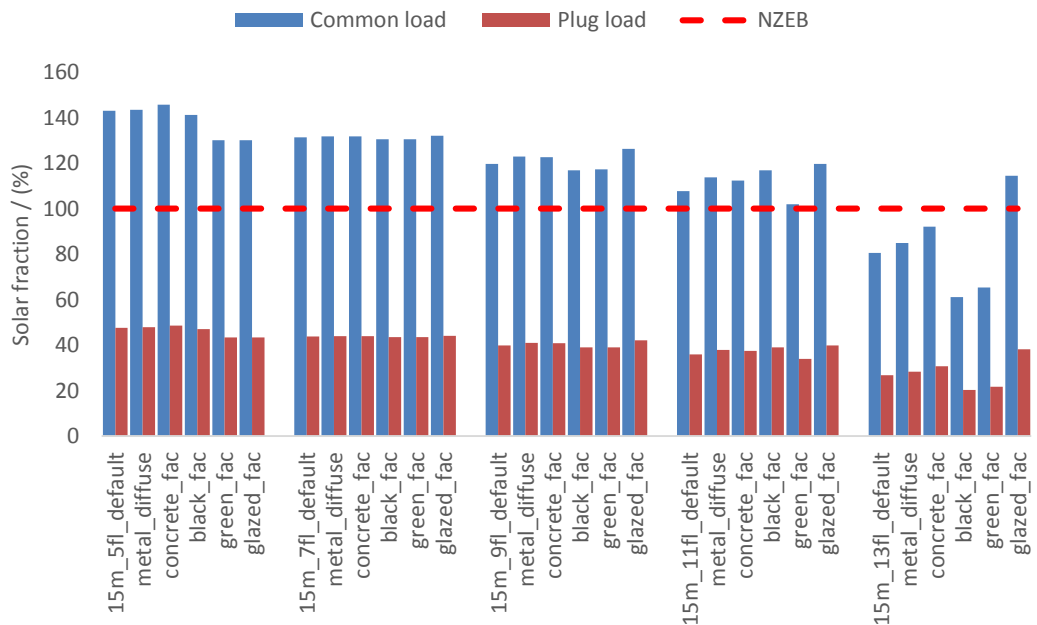

Figure 4.15 Solar fraction for different facade materials irradiation for a threshold 650 kWh/m^{2}a

If the solar irradiation threshold is considered to be above 800 kWh/m^{2}a, then, firstly the suitable areas are reduced as the height of the surrounding increases and secondly the more reflective materials show a greater effect when the surroundings are taller.
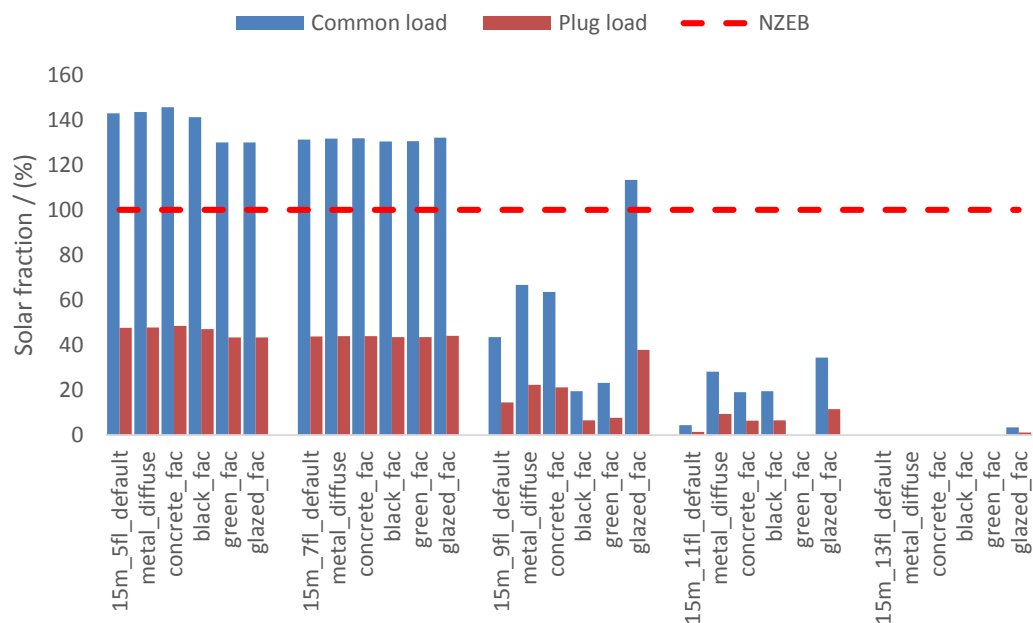
Figure 4.16 Solar fraction for different facade materials irradiation for a threshold 800 kWh/m^{2}a

The effect on the facades proved to be quite small and a reason for this could be the fixed orientation that this study assumes. Since most of the useful irradiation comes from azimuths close to the absolute south, this irradiation is reflected on the north facade of the examined building, which still results in values lower than 650 kWh/m^{2}a. For this reason the southern façade, indicated as the one with most solar potential, does not show a significant change.

The effect on the irradiation for buildings higher than 7 floors indicate that materials with high reflectance such as the glazed façade, concrete plaster and metal façades increase the irradiation, while materials with lower reflectance such as the black absorptive, green and default facade show a reduction of the irradiation. However, if the threshold for suitable areas is set 650 kWh/m^{2}a, then SAFAR cannot detect this of more areas with lower or higher solar irradiation. Higher buildings appear to be more susceptible to reflect the sunlight. The more reflective surfaces increase the production potential of the examined building, in some cases extremely much, which could also be due to the fact that in the study all surrounding buildings were assumed to have a 100% coverage of the studied facade materials. This means that for larger areas of very reflective materials, the amount of reflected indirect sunlight is large. This however appears to be beneficial for the solar potential of the building, but introduces problems related to visual comfort in the building. On the other hand more absorptive

materials had a negative effect on the irradiation of the building, since less indirect solar radiation was transmitted.

4.2 Solar energy building assessment tool

In order to demonstrate the solar energy building assessment tool, an analysis of the solar potential ($SAFAR_n$), the electricity production of three different system setups and the load coverage on an annual and hourly basis was performed.

Figure 4.17 shows a visual representation of the solar potential assessment for all suitable and unsuitable building envelope areas. It is evident how the building surfaces are affected by self-shading (indicated by green colour) and shading from the neighbouring buildings. The building demonstrates a high solar irradiation on the roof and shows that all areas are suitable for the installation of PVs. As for the facade surfaces, only the south-facing facades receive an irradiation over 650 kWh/m²a and are considered suitable. The outcome of this result is very useful in terms of locating the surfaces that are appropriate for solar energy harvesting and the surfaces that are shaded or in general receive lower solar radiation.

North-East

North-West

South-East

South-West
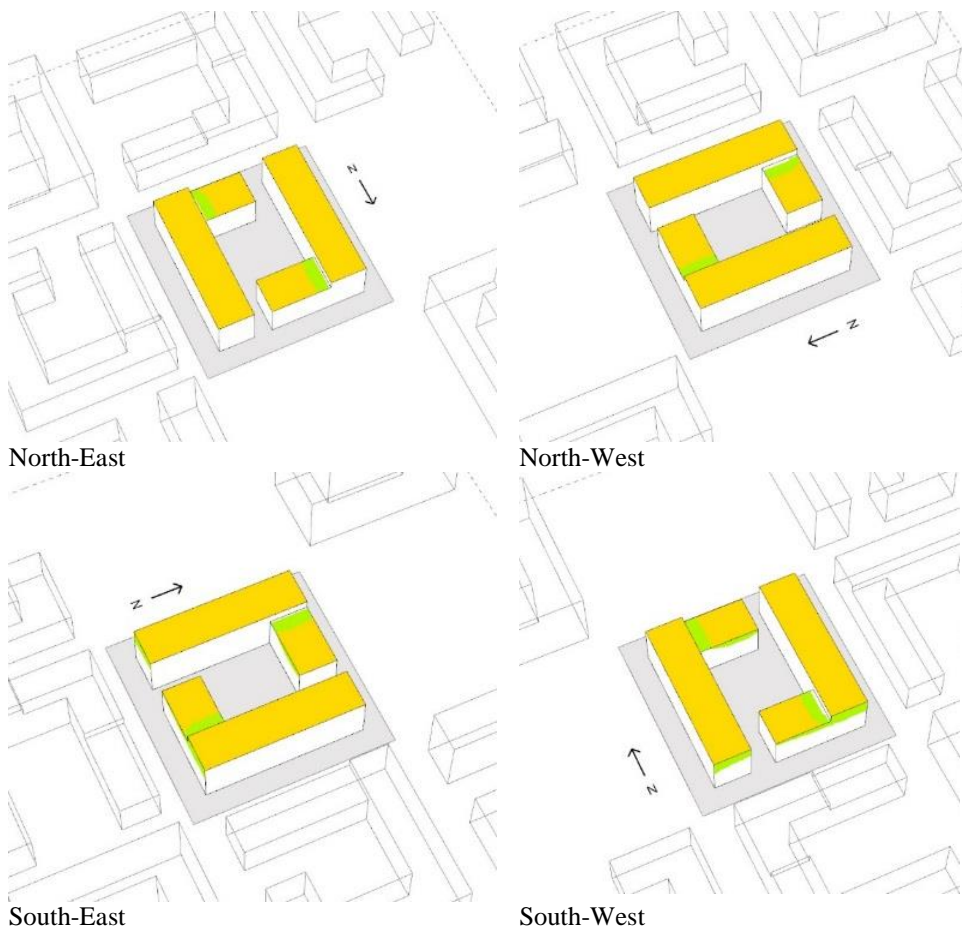
< 650 kWh/m²a	651 – 899 kWh/m²a	900 – 1020 kWh/m²a	> 1020 kWh/m²a

Figure 4.17 Colour mask for all suitable areas

The results regarding $SAFAR_n$, presented on Figure 4.18, demonstrate that the roof represents a much greater portion of the suitable area than the facades. The total value for $SAFAR_{650}$ is approximately 0.23.
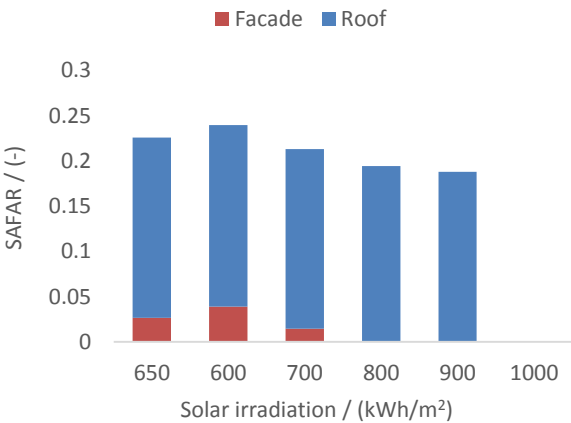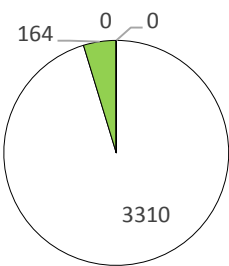

Figure 4.18 SAFARn for different irradiation values

The following charts (see Figure 4.19 and Figure 4.20) translate the $SAFAR_n$ coefficient into usable area in square meters. Due to the lack of any significantly higher building in the neighbouring context, 99% of the available roof surface area can be utilized, 93% of which receive irradiation higher than 900 kWh/m²a. As for the facade only 5% of the total facade area is suitable for installation of PV panels.
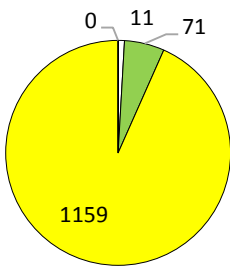
Figure 4.19 Roof area distribution   Figure 4.20 Facade area distribution
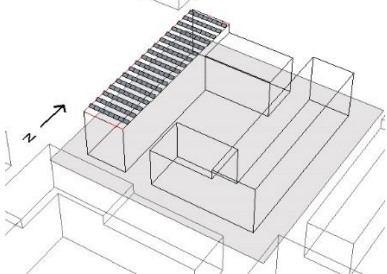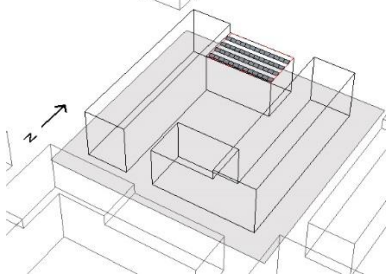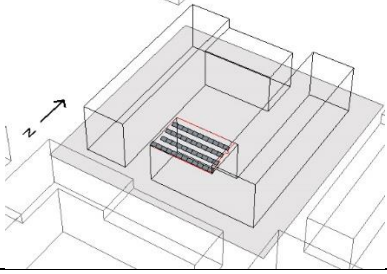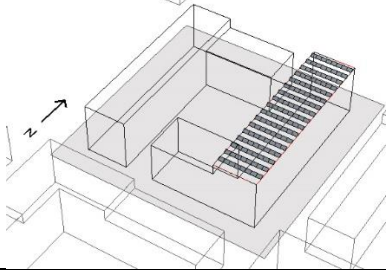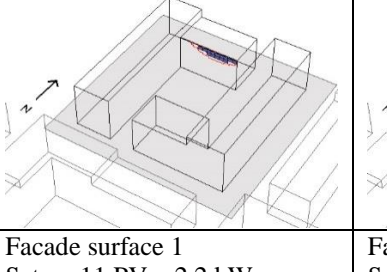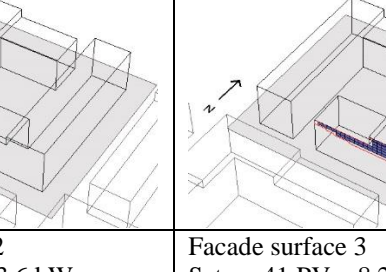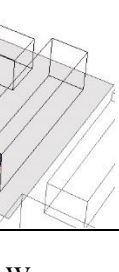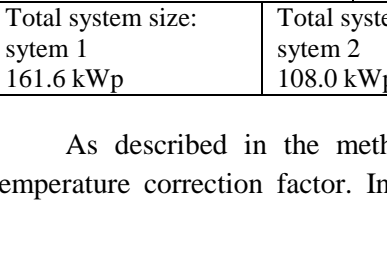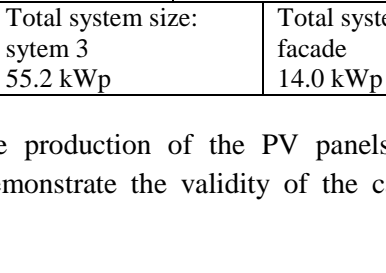
Table 4.2 shows the outcome of all generated system setups, according to the building surface, system setup size and number of panels. This information is particularly useful for

an estimation of the possible investment cost. Additionally, it also shows how the system would be fitted on the assigned surfaces. The system sizes were adapted according to the usable area of 75%, due to windows and roof installations, therefore, the images only show a visual representation of where and how the panels can be installed.

Table 4.2 Maximum number of panels and system size in kWp, for all roof and facade system setups

Setup 1: 0° inclination, 0m row spacing, 0° azimuth	Setup 2: 15° inclination, 0.5m row spacing, East-West	Setup 3: 30° inclination, 2m row spacing, 0° azimuth
Roof surface 1 Setup 1: 300 PV – 60.0 kWp Setup 2: 198 PV – 39.6 kWp Setup 3: 102 PV – 20.4 kWp	Roof surface 2 Setup 1: 117 PV – 23.2 kWp Setup 2: 78 PV – 15.6 kWp Setup 3: 34 PV – 6.8 kWp	
Roof surface 3 Setup 1: 91PV – 18.2 kWp Setup 2: 66 PV – 13.2 kWp Setup 3: 38 PV – 7.8 kWp	Roof surface 4 Setup 1: 300 PV – 60.0 kWp Setup 2: 198 PV – 39.6 kWp Setup 3: 102 PV – 20.4 kWp	
Facade surface 1 Setup: 11 PV – 2.2 kWp	Facade surfcae 2 Setup: 18 PV – 3.6 kWp	Facade surface 3 Setup: 41 PV – 8.2 kWp
Total system size: sytem 1 161.6 kWp	Total system size: sytem 2 108.0 kWp	Total system size: sytem 3 55.2 kWp	Total system size: facade 14.0 kWp

As described in the methodology, the production of the PV panels includes a temperature correction factor. In order to demonstrate the validity of the calculation, a

57

comparison was performed between the cell temperatures calculated by the tool, the cell temperature calculated in SAM and the ambient temperature for two systems on the roof and on the façade. Figure 4.21 shows the results for a system setup 1 for a system placed on the most exposed roof surface (surface 1, see Table 4.2). The cell temperature calculated by the tool, reaches maximum up to 45°C and generally could reach 50-55% difference from the ambient temperature. Due to the consideration of a sufficient air gap between the panel and the roof surface, the cell temperatures do not reach very high values that would affect the efficiency. Compared to SAM, the temperatures are slightly lower (4% average difference) and follow the same pattern of cell temperature rise and fall. This indicates that the calculation executes in correct manner and presents valid results.
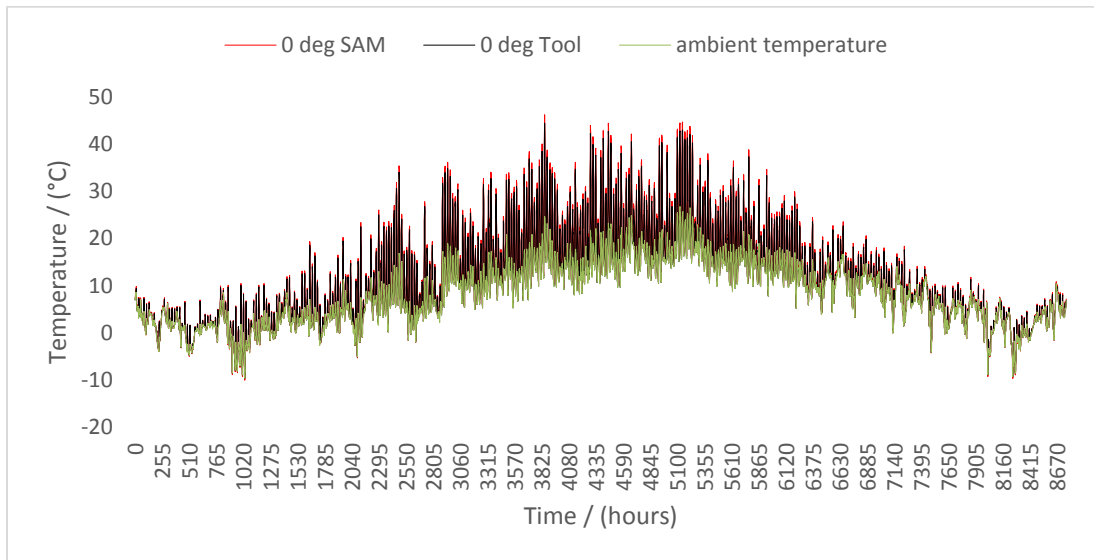
Figure 4.21 Ambient temperature versus cell temperature from SAM and the assessment tool for system setup 1

The cell temperature on the facade (see Figure 4.22), calculated by the tool results in higher temperatures, up to 55°C. Similarly to the previous simulation the cell temperature could reach 50-55% difference from the ambient temperature. Compared to SAM, the cell temperatures again do not differ significantly with an average difference of 3%. The reason for the higher temperature on the facade panels is the fact that they were assumed to be building-integrated. The calculation method for the temperature correction factor uses empirically-determined coefficients based on the type of module structure and mounting that take into account a smaller gap for air flow behind the panel.
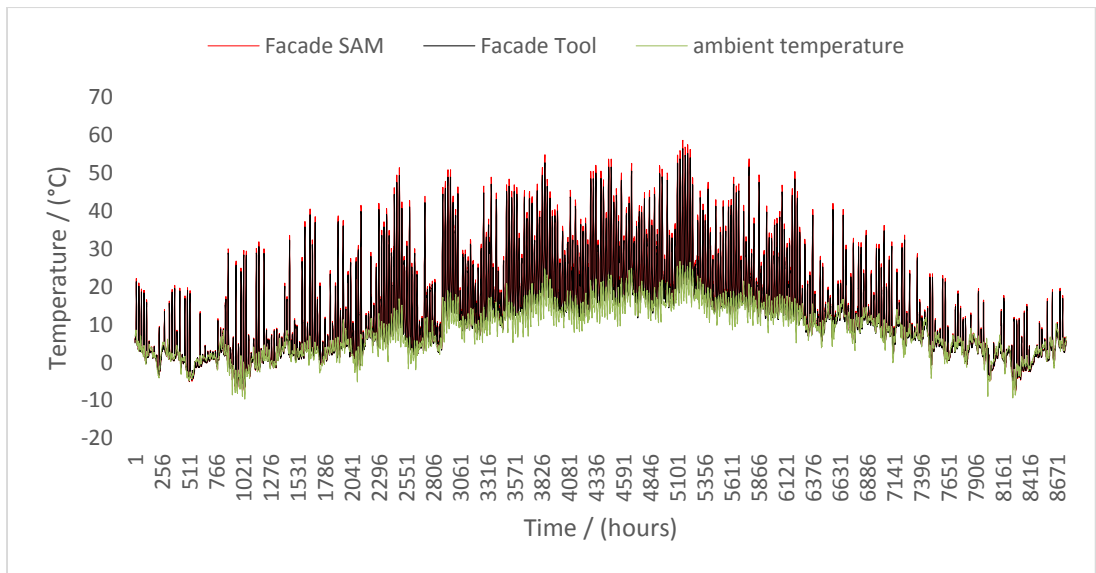
Figure 4.22 Ambient temperature versus cell temperature from SAM and the assessment tool for facade system

Figure 4.23 presents the hourly production output for system setups 1 and the consumption profiles for common and plug loads (see Appendix B for system 2, system 3 and facade system). The graphs indicate the maximum production that a system setup placed on all roof or facade surfaces can generate. Information is also provided on the annual solar fraction and the fraction of produced electricity to self-consumed electricity, which is useful in order to get an understanding of how much produced electricity is actually used in the building.

Figure 4.23 also demonstrates the hourly production and consumption profiles for a year for a system with 0 degrees inclination placed on all roof surfaces. The results (see also Table 4.3) indicate that annually the system can cover approximately twice the amount of common electricity load (228%), however, the actual utilization of the electricity in the building is 22%, which suggest that the rest of the produced electricity is either lost (if not possible to feed it into the city grid) or sold, which theoretically might not always be profitable in Sweden (Adolfsson & Hjerpe, 2014). Concerning the plug load, the system could cover up to 76% of the whole annual load, with a larger self-consumption fraction of 53%. It should be noted that one of the reasons for such a large production of this system is lack of mutual shading, since the panels are placed horizontally and are placed one next to each other, without any space, which allows for full area exploitation.
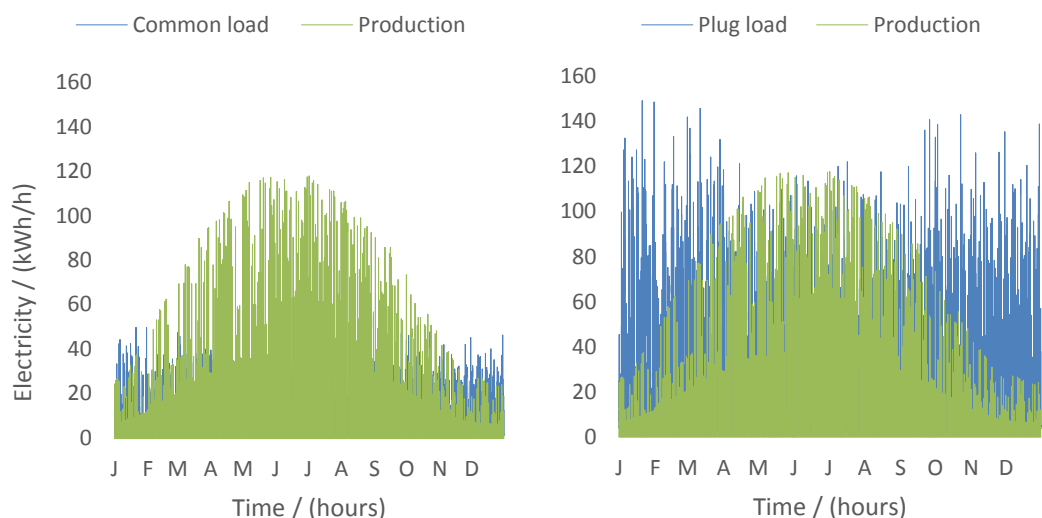
Figure 4.23 Production of system setup 1 (0 degrees) for all roof surfaces

Table 4.3 Solar fraction and Self-consumption fraction for common and plug loads

	Common load	Plug load
Solar fraction (%)	228	76
Self-consumed (%)	22	53

In order to provide flexibility in the tool, a function to choose which surfaces to install a PV system was provided. This way the PV potential can be assessed by defining only the surfaces that could cover enough electricity to cover the needs of the building and avoid too large overproduction. Table 4.4 shows that only placing a system on roof surface 1 (for reference see Table 4.2) is close to enough for covering the annual common load and would self-consume larger portion of its production than the system that is placed on all available roof surfaces (see also Table 4.3 and Table 4.4).

The outcome of this stage of the workflow would be useful for a calculation of the financial value of the saved electricity and the overall profitability of the system. This, however, was not a part of this study.

Table 4.4 Load match surface by surface for system setup 1

	Common load		Plug load	
	Solar fraction (%)	Self-consumed (%)	Solar fraction (%)	Solar fraction (%)
Roof surface 1	90	41	30	90
Roof surface 2	33	66	11	33
Roof surface 3	25	71	9	25
Roof surface 4	85	43	28	85

Finally, in order to validate the calculation of the hourly electricity production results, generated by the tool, a comparsion of all three roof systems is presented. For the system 1 (0 degrees system), the difference between the tool and SAM is approximatelly 6%, for system 2 (15 degrees), the difference is 9% and for system 3, a difference of 11% (see Figure 4.24, Figure 4.25 and Table 4.5). A source of this difference could be, as discussed in the method, the way the tool calculates the hourly irradiation. As mentioned, the middle panel of each row is taken and the same value is assumed for the all panels on the same row, which results in a slight overestimation of the results. Additionally, SAM takes into account more aspects of the PV system than the Grasshopper-based tool, which could lead to additioanl system losses and also be identified as a reason of the difference.
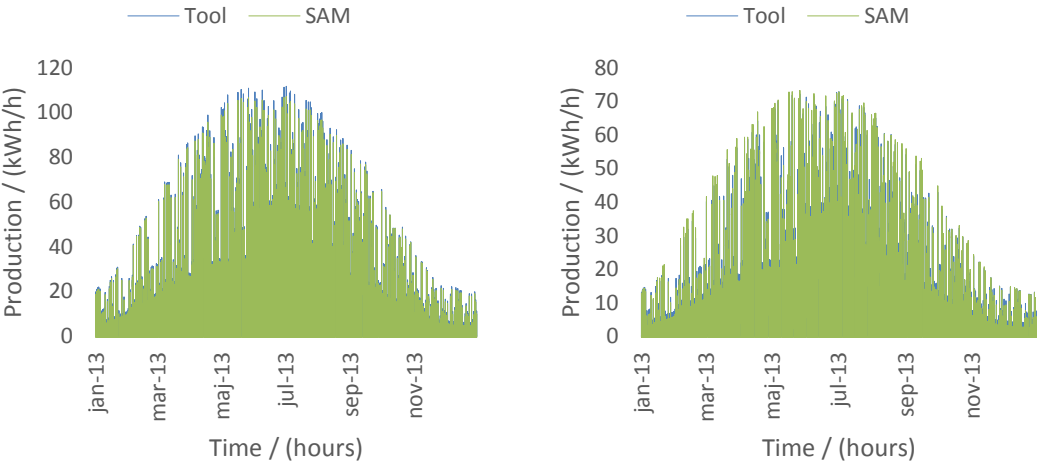
Figure 4.24 System 1 and system 2 production

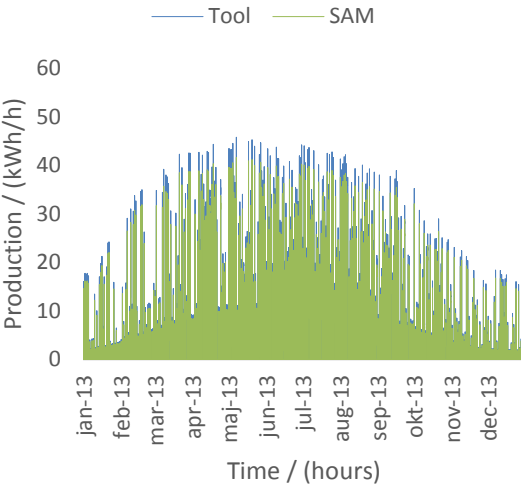Table 4.5 Results between SAM and the tool

Roof systems	System 1	System 2	System 3
Tool	141 091	55 589	92 534
SAM	132 781	50 587	82 655
Difference	6%	9%	11%

Figure 4.25 System 3 production

5   Conclusions

In this research $SAFAR_n$ solar potential metric was tested for the case of seven buildings in Hyllie, Malmö area in Southern Sweden. The results showed that only roof surfaces and south-facing facades or facades with an azimuth angle close to the absolute south could be considered suitable in this and similar latitude regions. However, due to the urban context the south façades were strongly affected. Moreover, the building density and compactness were identified as determining factors for the $SAFAR_n$ metric. Based on the results obtained from $SAFAR_n$, a good understanding was developed for some of affecting factors for the potential of a building to harvest solar energy. Additionally, a large potential for locally produced solar electricity was identified, as all buildings theoretically covered their common electricity need.

The research also examined the surroundings' effect on $SAFAR_n$ and the results showed that larger street dimensions are more favourable for the overall solar potential of buildings. Additionally, it became evident that the façades are the most affected by the height of the surrounding buildings. A large difference between the solar potential between $SAFAR_{650}$ and $SAFAR_{800}$ was identified considering the roof surface, where the difference in solar potential and potential for load coverage was significantly affected by the surroundings. If 800 kWh/m^2a as a suitable threshold for the roof was instead considered, surrounding buildings of no more than two floors higher than the examined building showed to be optimal for keeping the roof solar potential high. Furthermore, the study on different facade materials identified a significant contribution of high reflectance materials such as glazed facades and painted concrete. Other less reflective surfaces showed to have a slightly negative effect on the irradiation. The results of this study can be used to correctly determine the best building heights and street dimensions in order to optimize the solar potential of the building in an urban district.

In this study a Grasshopper-based building assessment tool for solar energy design during early design phase was developed and demonstrated by assessing a theoretical building in diverse urban surroundings. The tool is capable of performing predictions on solar potential ($SAFAR_n$), providing the user with a visual and numerical output of the results, generation of a solar energy system on any suitable surface, providing flexibility and choice of system setups. Additionally, the hourly PV output could provide useful information on the actual load coverage, as well as to assist with a financial benefit calculation of the selected system. The tool was validated by comparing the output to the validated solar energy system modelling program SAM and the results indicated a slight overestimation of the script, which are due to the complexity of SAM as a tool, as well as simplifications adopted in the calculation method of the Grasshopper-based tool.

The tool can be optimized by making it more user-friendly, also allowing for a simulation of each individual panel of the system in order to give a slightly more accurate result.

6 References

Adolfsson, M., Hjerpe, H. (2014). *Calculation model for LCC-analyses of photovoltaic systems in Sweden. The introduction of tax reduction as a subsidy*. Lund University.

Álvarez, J. R. (2013). *Energy and urban form: A top-down assessment tool*. Munich: PLEA2013.

Anderson, W.P., Kanaroglou, S.K., Miller, E.J. (1996). Urban Form, Energy and the Environment: A Review of Issues, Evidence and Policy. *Urban Studies 33*(1), 7-35.

Antonutto, G., McNeil, A. (2013). Radiance Primer. http://www.radiance-online.org/learning/tutorials/radiance-primer.pdf, Accessed 2015-05-05.

BBR (2015). *BBR – Boverkets byggregler.* http://www.boverket.se/sv/lag--ratt/forfattningssamling/gallande/bbr---bfs-20116/, Accessed 2015-03-03.

Beckman, J., Duffie, W. (1991). *Solar engineering of thermal processes*. New York: Whiley.

Bergström, H., Söderberg, S. (2008). Wind Mapping of Sweden: Summary of results and methods used. Elforsk.

Bernardo, R. (2013). *Retrofitted Solar Domestic Hot Water System for Single-Family Electrically-Heated Houses*. Lund: Department of Architecture and Built Environment, Lund University.

Biesbroek, K., Klein, R., Versele A., Breesch, H. (2010). *Design processes for net zero energy buildings.* Maastricht: SB 2010 conference on sustainable buildings.

Cheng, V., Steemers, K., Montavon, M., Compagnong, R. (2006). *Urban Form, Density and Solar Potential*. Geneva: PLEA 2006.

Compagnon, R. (2004). Solar and daylight availability in the urban fabric. *Energy and Buildings 36*(4), 321-328.

European Parliament (2010). *Directive 2010/31/EU of the European Parliament and of the Council*. http://eur-lex.europa.eu/legal-content/EN/TXT/PDF/?uri=CELEX:32010L0031&from=EN, Accessed 2015-04-15.

Gomes, J., Diwan, L., Bernardo, R., Karlsson, B. (2013). Minimizing the Impact of Shading at Oblique Solar Angles in a Fully Enclosed Asymmetric Concentrating PVT Collector. *2013 ISES Solar World Congress, Energy Procedia 57*, 2176-2185.

Grasshopper3d (2015). *About Grasshopper*. http://www.grasshopper3d.com/, Accessed 2015-04-15.

Hyllie (2015). *Hyllie - a new city district between Malmö and Copenhagen.* http://www.hyllie.com/in-english.aspx, Accessed 2015-04-30.

IEA (2013). *Transition to Sustainable Buildings: Strategies and Opportunities to 2050*. http://www.iea.org/publications/freepublications/publication/Building2013_free.pdf, Accessed 2015-03-10.

IEA (2015). *Task 51 IEA-SHC*. http://task51.iea-shc.org/, Accessed 2015-01-20.

IEA-PVPS (2014). *Trends 2014 in Photovoltaic Applications*. http://www.iea-pvps.org/index.php?id=3, Accessed 2015-01-20.

IEA-SHC (2015). *International Energy Agency - Solar Heating and Cooling Programme*. http://iea-shc.org/, Accessed 2015-04-05.

IEA-SHC Task 41 (2013). *Designing Photovoltaic Systems for Architectural Integration*. http://task41.iea-shc.org/data/sites/1/publications/task41A3-2-Designing-Photovoltaic-Systems-for-Architectural-Integration.pdf, Accessed 2015-03-11.

Intelligent Energy Europe (2012). *Home*. http://www.polis-solar.eu/, Accessed 2015-02-15.

Jakubiec, J.A., Reinhart, C. F. (2011). *DIVA 2.0: Integrating daylight and thermal calculations using Rhinoceros 3D, DAYSIM and EnergyPlus*. Sydney: Proceedings of Building Simulation 2011: 12th Conference of International Building Performance Simulation Association.

Jakubiec, J.A., Reinhart, C.F. (2013). A Method for Predicting City-Wide Electricity Gains from Photovoltaic Panels Based on LiDAR and GIS Data Combined with Hourly Daysim Simulations. *Solar Energy 93*, 127-143.

Kanters, J. (2015). *Planning for solar buildings in urban environments: An analysis of the design process, methods and tools*. Lund: Division of Energy and Building Design, Department of Architecture and Built Environment, Lund University

Kanters, J., Davidsson, H. (2014). Mutual shading of PV modules on flat roofs: a parametric study. *2013 ISES Solar World Congress, Energy Procedia 57*, 1706-1715.

Kanters, J., Dubois, M.-C., Wall, M. (2012a). Architects' design process in solar-integrated architecture in Sweden. *Architectural Science Review 56*(2), 141-151.

Kanters, J., Horvat, M. (2012). The Design Process known as IDP: A Discussion. *Energy Procedia 30*, 1153-1162.

Kanters, J., Horvat, M., Dubois, M.-C. (2012b). Tools and methods used by architects for solar design. *Energy and Buildings 68*, 721-731.

Kanters, J., Wall, M. (2014). The impact of urban design decisions on net zero energy solar buildings in Sweden. *Urban, Planning and Transport Research: An Open Access Journal 2*(1), 312-332.

Kanters, J., Wall, M., Kjellsson, E. (2014). The solar map as a knowledge base for solar energy use. *Energy Procedia 48*, 1597-1606.

King, D. L., Boyson, W. E., Kratochvil, J. A. (2004). *Photovoltaic Array Performance Model*. Sandia National Laboratories.

Larsvall, M., Teder, M., Engdahl, B., Carlsson, C. (2010). *Reflexioner över Stadsplaneringens Vardagsfrågor*. Malmö: Malmö stad.

McNeel (2015). *Robert McNeel & Associates*. http://www.en.na.mcneel.com/, Accessed 2015-04-04.

Nguyen, H.T., Pearce, J.M., Harrap, R., Barber, G. (2012). The Application of LiDAR to Assessment of Rooftop Solar Photovoltaic Deployment Potential in a Municipal District Unit. *Sensors 12*, 4534-4558.

NREL (2015). *System Advisor Model (SAM)*. https://sam.nrel.gov/, Accessed 2015-05-11.

O'Brien, W., Kennedy1, C., Athienitis, A. and Kesik, T. (2010) The relationship between personal net energy use and the urban density of solar buildings. *Environment and Planning B: Planning and Design 37*(6), 1002 – 1021.

Pless, S., Torcellini, P. (2010). Net-Zero Energy Buildings: A Classification System Based on Renewable energy Supply Options. Denver: NREL.

PVGIS (2015). *Photovoltaic Geographical Information System* (PVGIS). http://re.jrc.ec.europa.eu/pvgis/, Accessed 2015-04-20.

Robinson, D., Stone, A. (2004). *Irradiation modelling made simple: the cumulative sky approach and its applications*. Eindhoven: PLEA2004 - the 21st Conference on Passive and Low Energy Architecture.

Roudsari, M. S., Pak, M., Smith, A. (2013). *Ladybug: A Parametric Environmental Plugin for Grasshopper to Help Designers Create an Environmentally-Conscious Design*. Chambery: IBPSA.

Sartori, I., Napolitano, A., Voss, K. (2012). Net zero energy buildings: A consistent definition framework. *Energy and Buildings 48*, 220-232.

Sattrup, P. A., Strømann-Andersen, J. (2013). Building typologies in Northern European cities: daylight, solar access and building energy use. *Journal of Architectural and Planning Research 30*(1).

SCN (2012). *Kravspecifikation för nollenergihus, passivhus och minienergihus. Bostäder*. http://www.nollhus.se/dokument/Kravspecifikation%20FEBY12%20-%20bostader%20sept.pdf, Accessed 2015-05-06.

SVEBY (2012). *Brukarindata bostäder.* http://www.sveby.org/wp-content/uploads/2012/10/Sveby_Brukarindata_bostader_version_1.0.pdf, Accessed 2015-02-25.

Swedish Energy Agency (2013). *Energy in Sweden 2013*. Bromma: Arkitektkopia.

UN (2014). *World Urbanization Prospects: Highlights*. http://esa.un.org/unpd/wup/Highlights/WUP2014-Highlights.pdf, Accessed 2015-04-23.

University of California (1998). *Setting Rendering Options*. http://radsite.lbl.gov/radiance/refer/Notes/rpict_options.html, Accessed 2015-03-03.

van Esch, M., Looman, R., de Bruin-Hordijk, G. (2012). The effects of urban and building design parameters on solar access to the urban canyon and the potential for direct passive solar heating strategies. *Energy and Buildings 47*, 189-200.

Ward, G., Shakespear, R. (1998). Chapter 6: Daylight simulations. In: *Rendering with Radiance: The Art and Science of Lighting Visualizations*. San Francisco: Morgan Kaufmann Publishers, 341-390.

Appendix A: SAFAR$_n$ Grasshopper-based script
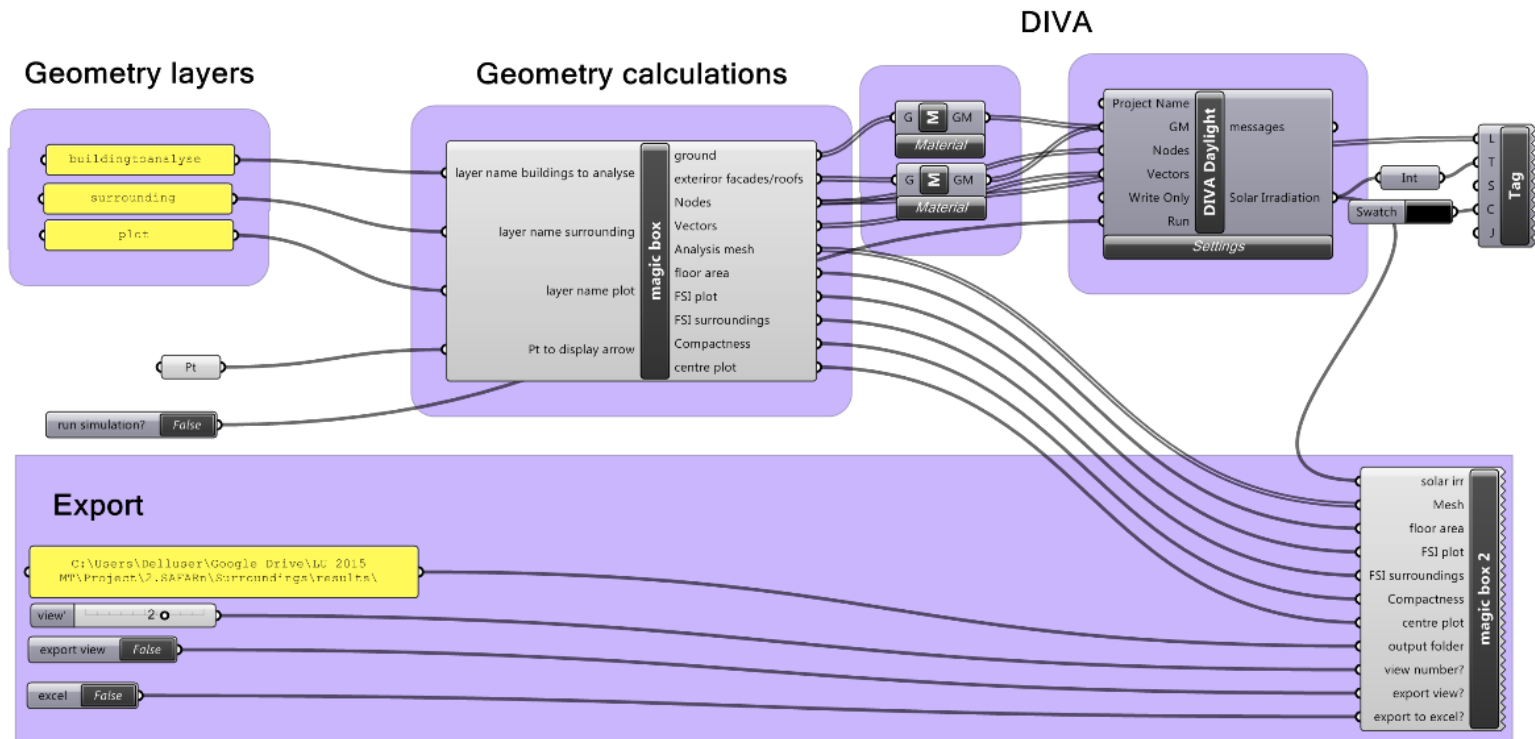
Appendix B: Hourly production

The following figures show the hourly values of system 2, system 3 and the facade PV systems. The annual solar fraction and the self-consumption ratio are also shown
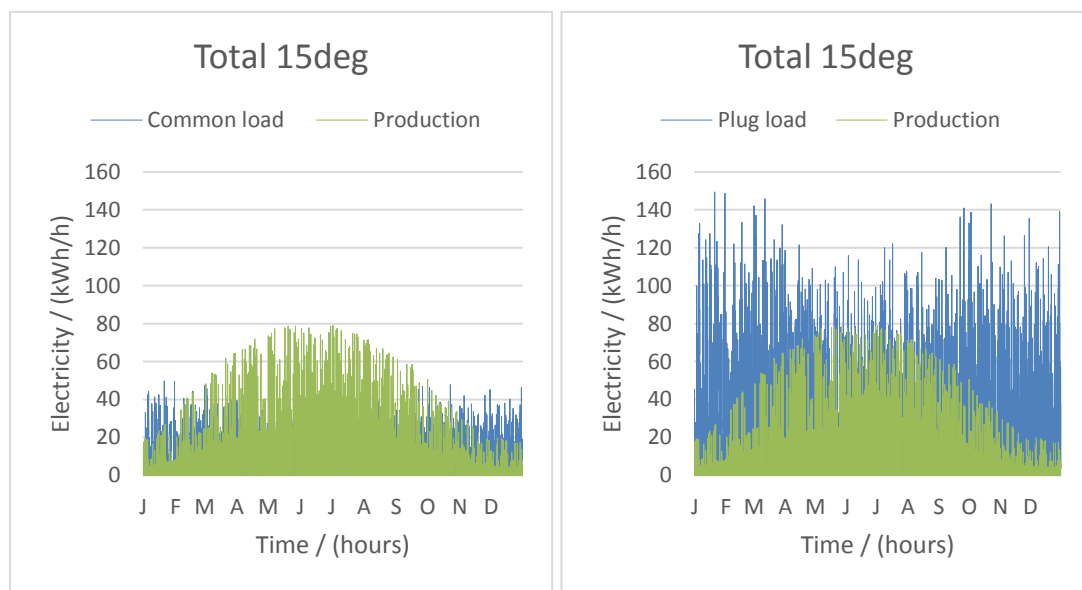
	Common load	Plug load
Solar fraction (%)	150	50
Self-consumed (%)	29	57

Load match surface by surface for system setup 2

	Common load		Plug load	
	Solar fraction	Self-consumed	Solar fraction	Self-consumed
Roof surface 1	0.54	0.56	0.18	0.14
Roof surface 2	0.22	0.71	0.07	0.06
Roof surface 3	0.18	0.78	0.06	0.06
Roof surface 4	0.55	0.52	0.18	0.14

Total facade — Common load / Production (left); Total facade — Common load / Production (right)
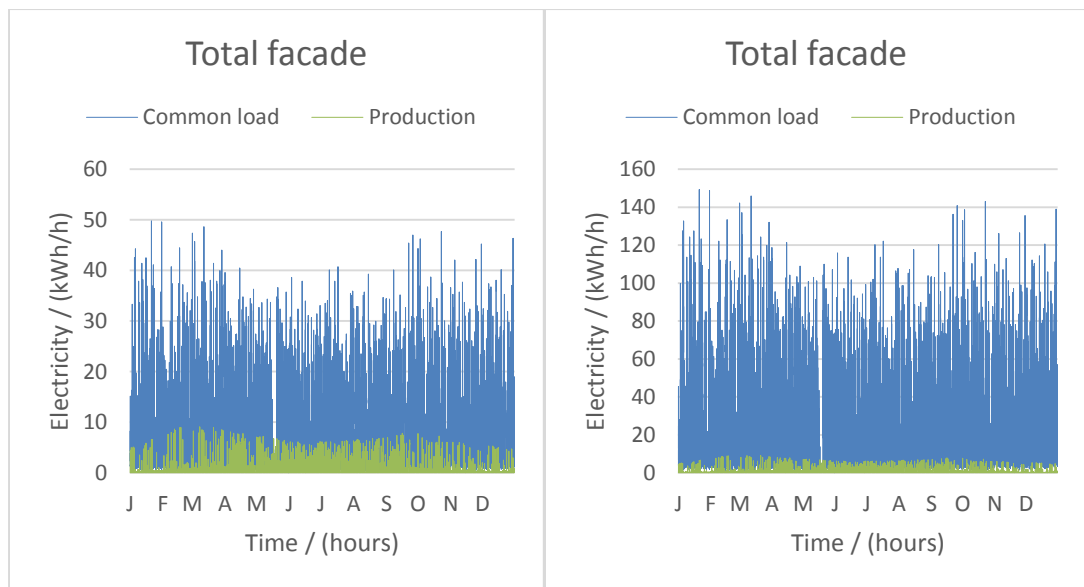
	Common load	Plug load
Solar fraction	0.14	0.04
Self-consumed	0.78	0.91

Load match surface by surface for facade systems

	Common load		Plug load	
	Solar fraction	Self-consumed	Solar fraction	Self-consumed
Facade surface 1	0.02	0.98	0.01	0.99
Facade surface 2	0.03	0.93	0.01	0.99
Facade surface 3	0.08	0.85	0.03	0.99

30 deg — Common load / Production (left); 30 deg — Plug load / Production (right)
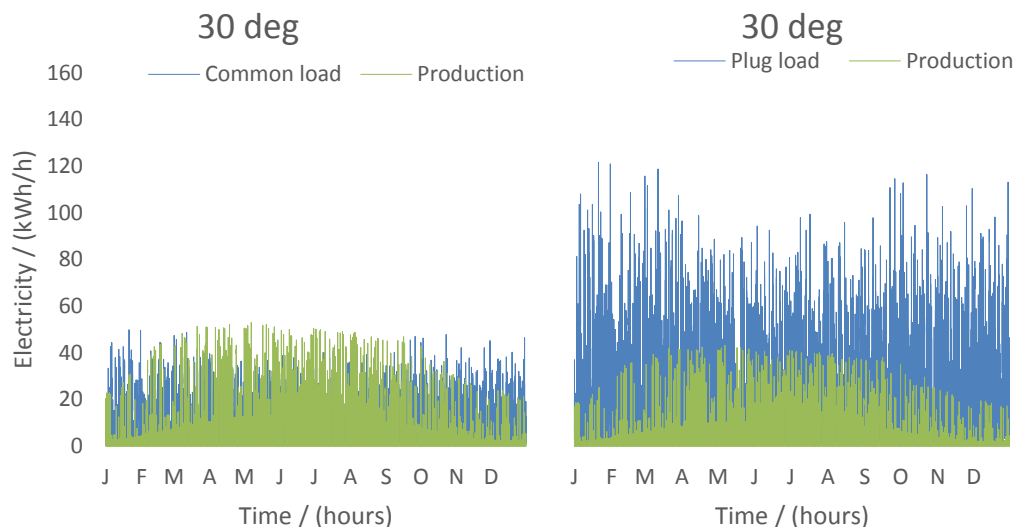
Production of system setup 3 (30 degrees) for all roof surfaces

Solar fraction and Self-consumption fraction for common and plug loads

	Common load	Plug load
Solar fraction (%)	90	40
Self-consumed (%)	30	67

Load match surface by surface for system setup 3

	Common load		Plug load	
	Solar fraction	Self-consumed	Solar fraction	Self-consumed
Roof surface 1	0.33	0.65	0.11	0.82
Roof surface 2	0.11	0.82	0.04	0.94
Roof surface 3	0.13	0.80	0.04	0.93
Roof surface 4	0.33	0.65	0.11	0.82
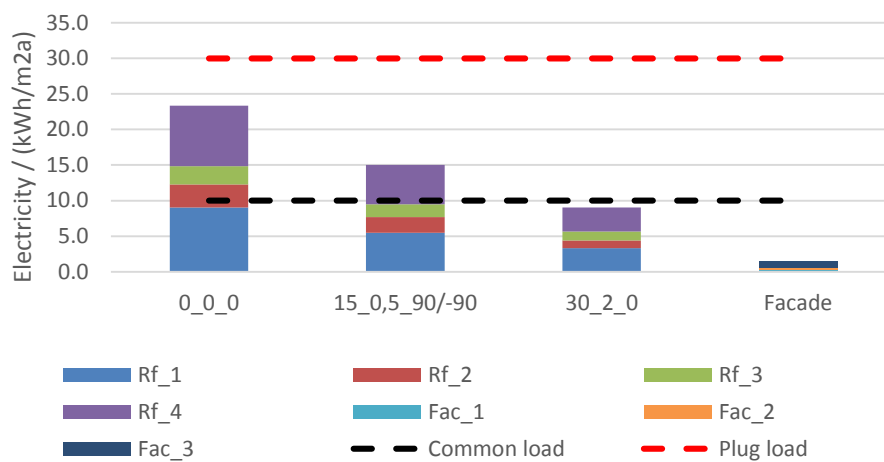
Cumulative production, based on hourly simulation for all systems and all surfaces

LUND UNIVERSITY

Dept of Architecture and Built Environment: Division of Energy and Building Design
Dept of Building and Environmental Technology: Divisions of Building Physics and Building Services